The diversity of Triassic South American sphenodontians: a new basal form, clevosaurs, and a revision of rhynchocephalian phylogeny

Sofia A. V. Chambi-Trowell, Agustín G. Martinelli, David I. Whiteside, Paulo R. Romo de Vivar, Marina Bento Soares, Cesar L. Schultz, Pamela G. Gill, Michael J. Benton & Emily J. Rayfield

View supplementary material 🖺

Published online: 01 Nov 2021.

Submit your article to this journal 🖉

View related articles 🗗

View Crossmark data 🗗

Taylor & Francis
Taylor & Francis Group

Check for updates

The diversity of Triassic South American sphenodontians: a new basal form, clevosaurs, and a revision of rhynchocephalian phylogeny

Sofia A. V. Chambi-Trowell[a]* (iD), Agustín G. Martinelli[b] (iD), David I. Whiteside[a,c] (iD),
Paulo R. Romo de Vivar[d] (iD), Marina Bento Soares[d,e] (iD), Cesar L. Schultz[d,f] (iD), Pamela G. Gill[a,c] (iD),
Michael J. Benton[a] (iD) and Emily J. Rayfield[a] (iD)

[a]*School of Earth Sciences, University of Bristol, Bristol, BS8 1TF, UK;* [b]*CONICET – Sección Paleontología de Vertebrados, Museo Argentino de Ciencias Naturales 'Bernardino Rivadavia', Av. Ángel Gallardo 470, Buenos Aires, C1405DJR, Argentina;* [c]*Department of Earth Sciences, Natural History Museum, Cromwell Road, London, SW7 5BD, UK;* [d]*Programa de Pós-Graduação em Geociências, Instituto de Geociências, Universidade Federal do Rio Grande Do Sul, Avenida Bento Gonçalves 9500, Agronomia, Porto Alegre, RS, 91501-970, Brazil;* [e]*Departamento de Geologia e Paleontologia, Museu Nacional, Universidade Federal do Rio de Janeiro, Quinta da Boa Vista s/n, São Cristóvão, Rio de Janeiro, RJ, 20940-040, Brazil;* [f]*Laboratório de Paleontologia de Vertebrados, Universidade Federal do Rio Grande do Sul, Porto Alegre, Brazil*

Rhynchocephalians are a group of lizard-like diapsid reptiles that were very diverse during the Mesozoic but are now restricted to a single extant genus in New Zealand. Recent cladistic analyses have revealed two major clades, Eusphenodontia and the more crownward Neosphenodontia, but relationships of individual taxa have remained difficult to determine because of missing data and an unrevised data matrix. Here we drastically revise the established data matrix on rhynchocephalians by reassessing, evaluating, and adding new characters and operational taxonomic units, differing from any previous analyses in our goal to consider all known rhynchocephalians. In addition, we describe a new genus and species of an early eusphenodontian taxon from the Norian of southern Brazil, with a unique mosaic of plesiomorphic and apomorphic traits, and we re-examine the craniodental anatomy of the eusphenodontian *Clevosaurus brasiliensis* with μCT imaging, revealing a unique form of acrodonty amongst rhynchocephalians.

http://zoobank.org/urn:lsid:zoobank.org:pub:A9211C5A-D4F9-472A-B8AB-877D13ABFDD5

Introduction

Rhynchocephalia, a diapsid lizard-like group of reptiles and sister group to Squamata, was diverse and globally distributed during most of the Mesozoic but is now represented by a single genus in New Zealand (Hay *et al.* 2010). The earliest diverging rhynchocephalian taxa, such as *Gephyrosaurus* and *Diphydontosaurus* (Evans 1980; Whiteside 1986), had at least in part pleurodont dentition, but later forms were fully acrodont, some of the oldest of which are known from the Late Triassic of South America. There have been considerable efforts to reconstruct the phylogeny of the rhynchocephalians, but results have been mixed.

South America yields a quite remarkable record of Triassic rhynchocephalians, with specimens known from the late Carnian to early Norian of the Santa Maria Supersequence (Zerfass *et al.* 2003; Bonaparte & Sues 2006; Horn *et al.* 2014; Schultz *et al.* 2020) of southern Brazil, and the middle Norian to late Rhaetian of

western Argentina (Martínez *et al.* 2013; Apesteguía 2016). The Brazilian fossils are *Clevosaurus hadroprodon* (Hsiou *et al.* 2019, but see Supplemental material) and an indeterminate genus and species based on an isolated palatine (Romo-de-Vivar-Martínez *et al.* 2021), both from the late Carnian *Hyperodapedon* Assemblage Zone (AZ) at the base of the Candélaria Sequence. Two more taxa, *Clevosaurus brasiliensis* (Bonaparte & Sues 2006) and *Lanceirosphenodon ferigoloi* (Romo de Vivar *et al.* 2020a) from the early Norian *Riograndia* AZ, occur at the top of the Candelária Sequence (Schultz *et al.* 2020). The record from Argentina includes a specimen mentioned briefly from the mid-to-late Norian Los Colorados Formation, Ischigualasto-Villa Unión Basin (Apesteguía 2016), and *Sphenotitan leyesi* from the late Rhaetian Quebrada del Barro Formation, Marayes-El Carrizal Basin (Martínez *et al.* 2013). *Clevosaurus brasiliensis* and *Sphenotitan leyesi* are the most abundant components within their respective

---

*Corresponding author. Email: sc14927@bristol.ac.uk

faunal associations (Bonaparte *et al*. 2010; Martínez *et al*. 2013; Romo de Vivar *et al*. 2020a).

Here, we present two South American rhynchocephalian taxa in detail, based on specimens from the Late Triassic *Riograndia* AZ of the Candelária Sequence (early Norian, Late Triassic) of southern Brazil and excellent µCT scan data. First, we describe the cranial anatomy of the early eusphenodontian *Clevosaurus brasiliensis* based on three skulls (including its holotype) and review the material in the literature attributed to this taxon. Second, we describe a new rhynchocephalian genus and species. The holotype and referred specimens were formerly considered to be from juveniles of *Clevosaurus brasiliensis* (Bonaparte & Sues 2006; Romo de Vivar Martínez & Soares 2015), but we reidentify them as belonging to a new taxon based on their unique traits, after a review of the large collection of rhynchocephalians from this AZ (mainly represented by *Clevosaurus brasiliensis* material) at the Paleovertebrate Collection of the Universidade Federal do Rio Grande do Sul, Porto Alegre, Brazil. The evidence for the validity of the new taxon came initially from a morphometric analysis of the jaws of *Clevosaurus brasiliensis* (Romo de Vivar Martínez & Soares 2015) in which the supposed juveniles grouped separately. Since then, new µCT scans and detailed study of the cranial anatomy presented below demonstrate that it is a new genus and species with significant anatomical differences and lacking numerous apomorphies of *Clevosaurus*.

Our detailed anatomical studies of the two taxa have allowed us to consider the wider relationships of the South American rhynchocephalians. There have been a number of phylogenetic analyses of Rhynchocephalia in recent years, but these have been dominated by a more-or-less shared data matrix (e.g. Apesteguía & Novas 2003; Apesteguía & Carballido 2014; Apesteguía *et al*. 2014; Hsiou *et al*. 2015; Herrera-Flores *et al*. 2018; Romo de Vivar *et al*. 2020a; Simões *et al*. 2020), and all analyses met similar problems of poor resolution and poor support values because of incompletely coded taxa. We were able to cross-check and substantially add to the character list and include rhynchocephalian taxa that had never been included in phylogenetic analyses before, and so develop a more comprehensive analysis than previously attempted.

Repository abbreviations

NHMUK-PV, Palaeovertebrate Collection, Natural History Museum UK. **SNSB-BSPG**, Staatliche Naturwissenschaftliche Sammlungen Bayerns, Bavarian State Collection for Palaeontology and Geology. **UFRGS-PV**, Paleovertebrate Collection, Universidade Federal do Rio Grande do Sul, Porto Alegre, Rio Grande do Sul, Brazil. **UFSM-PV**, Paleovertebrate Collection, Universidade Federal de Santa Maria.

Material and methods

Materials

The fossil material used for this study comprises four nearly complete skulls, three belonging to *Clevosaurus brasiliensis* (holotype UFRGS-PV-0748-T, UFRGS-PV-0974-T, UFSM-PV-0131) and the holotype specimen (UFRGS-PV-0972-T) of a new genus and species. These skulls were subjected to µCT scanning at the University of Bristol using a Nikon XTH225ST CT scanner, with scan settings of 150 kVP, 175 µA, 1 s exposure and a copper filter of 0.5 mm, except for UFRGS-PV-0748-T, which used scan settings of 150 kVP, 46 µA, 1.415 s and no filter. Each of the four fossils used 3141 projections at an average of one frame per projection acquired during a full rotation of 360° and a source to detector distance of 1176 mm. UFSM-PV-0131 had a source to object distance of 88 mm, resulting in a 15.0 µm reconstructed voxel resolution; UFRGS-PV-0748-T had a source to object distance of 91 mm, resulting in a 18.9 µm reconstructed voxel resolution; UFRGS-PV-0972-T had a source to object distance of 86 mm, resulting in a 14.6 µm reconstructed voxel resolution; and UFRGS-PV-0974-T had a source to object distance of 111 mm, resulting in a 18.9 µm reconstructed voxel resolution. The scans were processed using Avizo Lite 9 (FEI Visualisation Sciences Group) to reconstruct segmented 3D models. Other specimens (e.g. UFRGS-PV-0848-T, UFRGS-PV-0827-T) were studied by first-hand examination.

Phylogenetic analysis

The phylogenetic analysis of the relationships of rhynchocephalians is based on the largest version of the traditional data matrix of Rhynchocephalia (49 operational taxonomic units, 73 characters) as revised by Romo de Vivar *et al*. (2020a), but further substantially modified here in terms both of operational taxonomic units (OTUs) and characters. We modified 29 characters, removed 14 and added 82 original characters of our own, in addition to one character from Rauhut *et al*. (2012), 17 characters from Simões *et al*. (2020), and three from Dupret (2004). This resulted in a matrix with a total of 162 characters.

We paid particular attention to the inclusion and exclusion of taxa in our data matrix. We noted that many of the previous analyses excluded several rhynchocephalians represented by fragmentary material, but

this had not been done in a consistent way. For example, some relatively more complete taxa (e.g. *Vadasaurus*, SNSB BSPG 1993 XVIII 3, *Colobops noviportensis*, *Tingitana* and the 'Kirtlington sphenodontian') have been ignored in favour of less complete taxa (e.g. *Fraserosphenodon*, *Kawasphenodon*, *Pelecymala*). Here, we address this problem by coding all known species of rhynchocephalians, in addition to unnamed species, that have been described in the literature. We strove to represent as many morphotypes as possible, considering all rhynchocephalians equally. We then: (1) removed those that were considered problematic (see Supplemental material); (2) checked for redundancy in coded taxa so that we still represent as many morphotypes as possible; and (3) identified and removed rogue taxa before analysis began. Unlike Romo de Vivar Martínez *et al.* (2020a), we chose not to include *Homoeosaurus* cf. *maximiliani* as there may be multiple species of *Homoeosaurus* besides *H. maximiliani*, and there is not sufficient description in the literature to differentiate them. We also combined the three Chinese clevosaurs into one OTU as it is unclear whether they represent separate species (see Jones 2006). See Supplemental materials for discussion of taxa that were not included.

Our initial matrix comprises 79 taxa (76 rhynchocephalians and three outgroups), where previously the largest number in a phylogenetic analysis was 47 (Romo de Vivar Martínez *et al.* 2020a, prior to removal of rogue taxa). We studied the South American taxa (including *Lanceirosphenodon ferigoloi*) first-hand, in addition to seven British taxa (see Supplemental material for more information). Other taxa were re-evaluated through a combination of literature review and high-resolution photography and unpublished images provided by the institutions holding certain specimens.

Prior to analysis, we checked our matrix of 79 OTUs and 162 characters in PAUP 4.0 (Swofford 2002) to identify redundant taxa – those that share >99% of their characters. This eliminated 17 taxa, reducing the number of taxa to 62 OTUs and rendering characters 13 and 130 as parsimony uninformative. We then checked the reduced matrix in TNT v. 1.5 (Goloboff & Catalano 2016) to identify and remove rogue taxa using the iterPCR protocol, namely *Whitakersaurus bermani*, *Deltadectes elvetica* and *Kawasphenodon expectatus*. The final matrix therefore had 59 OTUs, of which 56 were rhynchocephalians and three were outgroups, and 160 parsimony-informative characters. See Supplemental material and Supplemental Fig. 3.

We rooted the trees with three outgroups, the lepidosauromorph *Sophineta cracoviensis* (Evans & Borsuk-Białynicka 2009) and two extant squamates, the gecko

Aeluroscalabotes felinus Günther, 1864 and the iguanian *Pristidactylus torquatus* Philippi & Landeck, 1861, the latter having been used in previous phylogenetic analyses (Hsiou *et al.* 2015; Herrera-Flores *et al.* 2018). We chose to replace the previously used outgroup *Eichstaettisaurus* with *Aeluroscalabotes* as the latter is an extant taxon that can be more completely coded.

The revised taxon–character matrix was analysed under equally weighted maximum parsimony using TNT v. 1.5 (Goloboff & Catalano 2016) and Bayesian inference using MrBayes v. 3.2 (Huelsenbeck & Ronquist 2001; Ronquist *et al.* 2012). All characters were considered as non-additive (unordered). The TNT parsimony search strategies started using a traditional heuristic search of 5000 replicates of Wagner tree followed by tree bisection and reconnection (TBR) as the branch swapping algorithm. The best trees obtained were subjected to a final round of TBR branch swapping to find all MPTs. The possible phylogenetic positions and clade robustness of all taxa were assessed with Bremer decay indices from TBR branch swapping (Bremer 1994). Bayesian analysis was run for 10^7 generations, sampling parameters every 1000 generations and the first 25% of sampled trees were discarded as burn-in. All recovered MPTs were then summarized in a strict and a 50% consensus (MRC) tree. A maximum clade credibility (MCC) tree was also generated (Supplemental Fig. 5) from the Bayesian analysis output. While the MCC tree has greater resolution, MRC trees are known to represent a lower proportion of incorrect nodes (O'Reilly & Donoghue 2018) and therefore it is the MRC tree we discuss here.

Systematic palaeontology

Lepidosauria Haeckel, 1866 (*sensu* de Queiroz & Gauthier 2020)
Rhynchocephalia Günther, 1867 (*sensu* Gauthier, Estes & de Queiroz 1988)
Sphenodontia Williston, 1925 (*sensu* Benton 1985)
Eusphenodontia Herrera-Flores, Stubbs, Elsler & Benton, 2018
Clevosaurus Swinton, 1939
Clevosaurus brasiliensis Bonaparte & Sues, 2006
(Figs 1–8, 14, 15; Supplemental Figs 1, 2, 4)

Holotype. UFRGS-PV-0748-T (Figs 1A–C, 2), originally described by Bonaparte & Sues (2006), is a nearly complete, articulated skull of an adult specimen, ~23 mm long and slightly dorsoventrally crushed. Many of the bones display cracks and some bones were presumably lost at the time of discovery or during

preparation, with the right vomer and much of the left vomer missing, as well as the paroccipital processes, and some of the posterior-most region of the right articular.

Additional specimens used here. UFSM-PV-0131 (Fig. 1C, D, Supplemental Fig. 1) is a nearly complete skull of length ∼31 mm, which has undergone some dorsoventral flattening. The contrast between bone and matrix is not high and details of the teeth are near impossible to distinguish. Much of the braincase is missing, but the fused left opisthotic and prootic are present, along with a fragment of the cultriform process and the right basioccipital process. UFRGS-PV-0974-T (Fig. 1E, F, Supplemental Fig. 2) is a near-complete skull, laterally crushed, ∼21 mm long, with markedly less worn teeth than the holotype and UFSM-PV-0131. Three cervical vertebrae are also present. The crushing has displaced and destroyed many of the roofing bones of this skull.

Locality and horizon. The Linha São Luiz outcrop (29°33′45″ S, 53°26′48″ W) is located about 1.5 km north-west of Faxinal do Soturno city, Rio Grande do Sul State, southern Brazil. Its fossil content is referred to the *Riograndia* AZ (Bonaparte *et al*. 2010; Soares *et al*. 2011; Martinelli *et al*. 2020). This location exposes the top of the Candelária Sequence (Santa Maria Supersequence) and corresponds to the base of traditional Caturrita Formation (Andreis *et al*. 1980). The fossils were obtained from massive, fine-grained sandstones, interpreted as deposited in a deltaic or fluvial environment (Horn *et al*. 2014). Based on zircon U-Pb analyses, the maximum depositional age of the fossil-bearing layers is Norian at ∼225.42 ± 0.37 Mya (Langer *et al*. 2018).

The Linha São Luiz outcrop has produced the procolophonian *Soturnia caliodon* (Cisneros & Schultz 2003), the rhynchocephalians *Clevosaurus brasiliensis* (Bonaparte & Sues 2006) and *Lanceirosphenodon ferigoloi* (Romo de Vivar *et al*. 2020a), the non-rhynchocephalian lepidosauromorph *Cargninia enigmatica* (Bonaparte *et al*. 2010; Romo de Vivar *et al*. 2020b), an archosaur of uncertain affinities, *Faxinalipterus minima* (Bonaparte *et al*. 2010; Soares *et al*. 2013), the dinosaur *Guaibasaurus candelariensis* (Bonaparte *et al*. 1999, 2007), and the probainognathian cynodonts *Brasilodon quadrangularis* (= *Brasilitherium riograndensis*, *Minicynodon maieri*), *Riograndia guaibensis* and *Irajatherium hernandezi* (e.g. Bonaparte *et al*. 2001, 2003, 2005, 2010, 2012; Martinelli *et al*. 2005, 2017; Oliveira *et al*. 2011; Soares *et al*. 2011).

Diagnosis (modified from Bonaparte & Sues 2006; Hsiou *et al*. 2015). A moderately sized rhynchocephalian with a skull 21–31 mm long, markedly short robust snout and broad skull, and with the following unique combination of features:

1. Acrodont teeth that extend deeply within the premaxillae, maxillae and dentaries, and thereby remain visible along the entire length of the tooth-bearing portions of the jaws even when worn flat.
2. Adult maxilla with two posteriorly positioned flanged teeth, followed distally by one or two smaller, sub-conical teeth.
3. Narrow and elongate palatine, bearing anteriorly a medially positioned cluster of small teeth, in addition to a single small tooth that is laterally displaced from the main palatine tooth row.
4. Interdigitation between the edges of the jugal and postorbital bones, the prefrontal and maxilla, and the pterygoid and palatines, rather than simple overlapping facets (Supplemental Fig. 4A–D).
5. Three longitudinal rows of teeth on the pterygoid, the lateral-most row consisting of just three to four teeth.
6. A near vertical symphysis (less than 120° in lateral view between the direction of the symphysis and the longitudinal axis of the mandible).
7. A pronounced edentulous region between the posterior-most dentary tooth (ultimate additional tooth) and the coronoid process.
8. The ultimate additional tooth on the dentary is significantly larger than all other dentary teeth and is mesiodistally elongated, with an anteriorly placed cusp when unworn.

Description

Skull. Among the three specimens examined here, almost all bones of the skull can be accounted for, with the exceptions of a complete vomer and a verifiable stapes.

Premaxilla. Each premaxilla (Fig. 3A, B) bears a single tooth that extends deep into the premaxillary bone, and which is more exposed on the lingual side as the bone is worn away by the occlusion of the lower jaw, forming a chisel-like edge. The presence of a single tooth on the premaxilla is a condition shared with *C. bairdi* (Sues *et al*. 1994) but it is less prominent here and nearly in line with the maxillary teeth. The nasal process is narrow and columnar but flattens mediolaterally where it comes into contact with the nasal. The maxillary process is as tall as the nasal process and is mediolaterally flattened and broad. As in the premaxillae of other *Clevosaurus* (Fraser 1988; Klein *et al*. 2015;
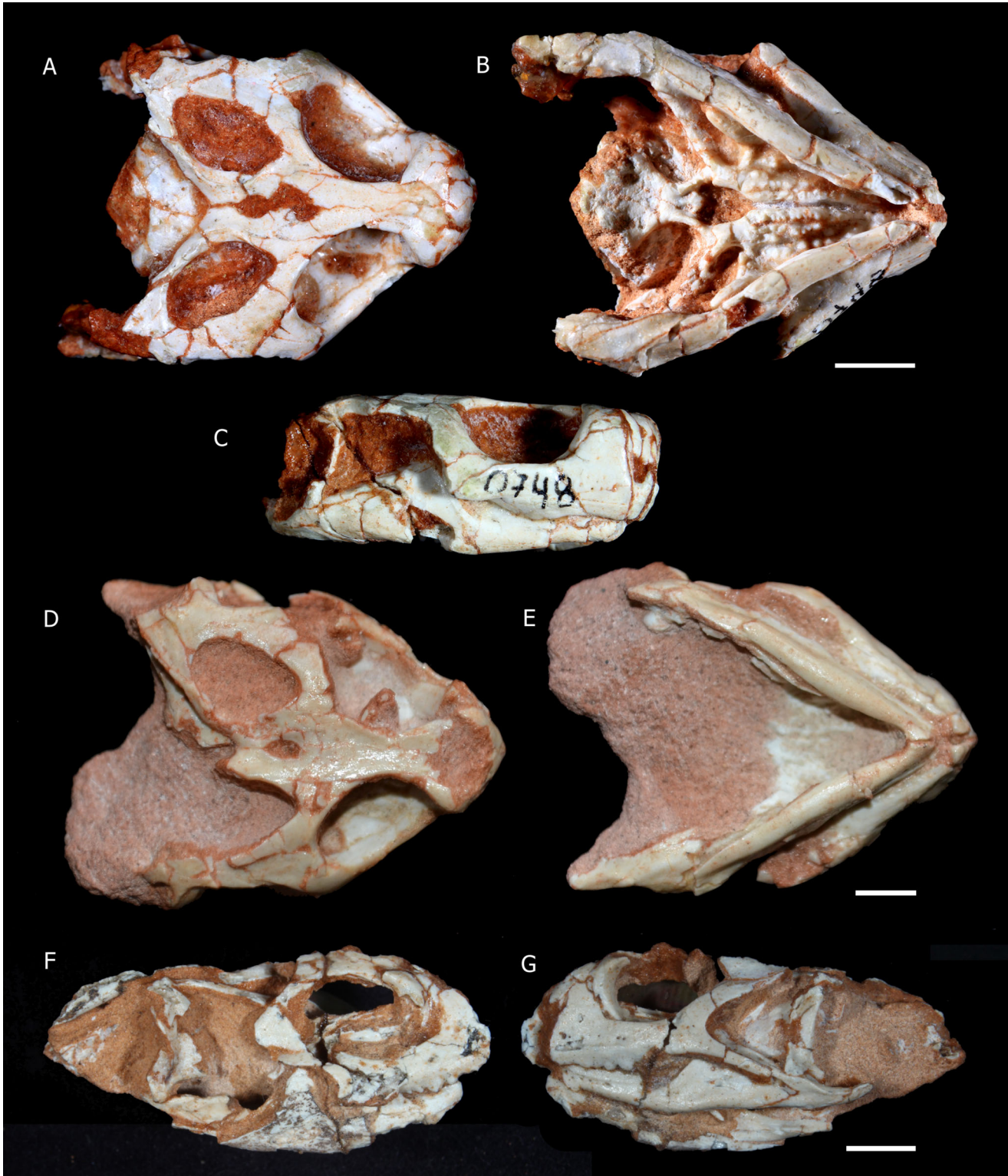
Figure 1. Cranial material of *Clevosaurus brasiliensis*. **A–C,** skull of UFRGS-PV-0748-T in: **A,** dorsal; **B,** ventral; and **C,** right lateral views. **D, E,** skull of UFSM-PV-0131 in **D,** dorsal; and **E,** ventral views. **F, G,** skull of UFRGS-PV-0974-T in: **F,** right lateral; and **G,** left lateral views. Scale bars equal 5 mm.
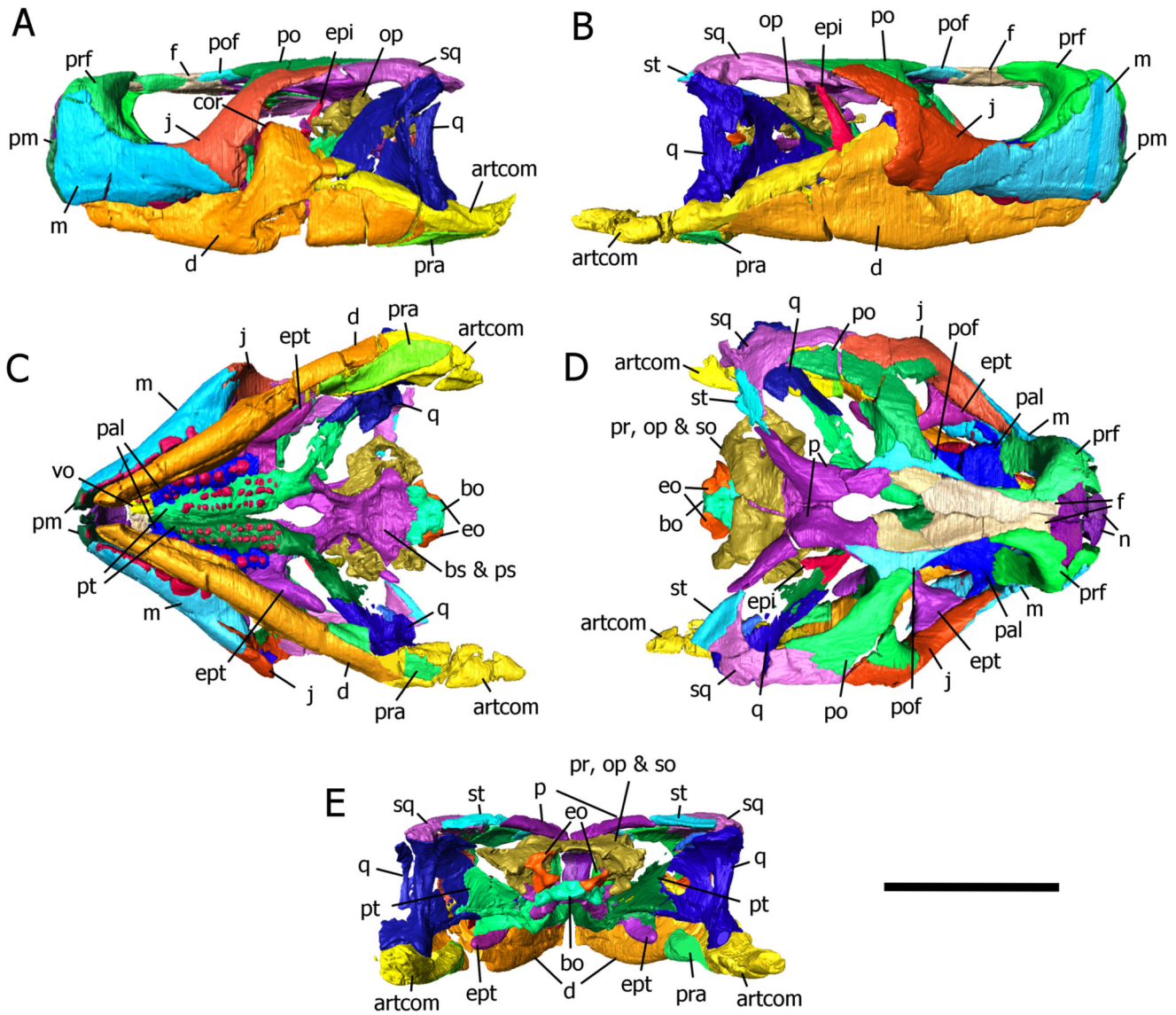
Figure 2. The digitally segmented holotype skull of *Clevosaurus brasiliensis* (UFRGS-PV-0748-T). **A,** left lateral; **B,** right lateral; **C,** ventral; **D,** dorsal; and **E,** posterior views. **Abbreviations: artcom**, articular complex; **bo**, basioccipital; **bs**, basisphenoid; **cor**, coronoid; **d**, dentary; **eo**, exoccipital; **epi**, epipterygoid; **ept**, ectopterygoid; **f**, frontal; **j**, jugal; **m**, maxilla; **n**, nasal; **op**, opisthotic; **p**, parietal; **pal**, palatine; **pm**, premaxilla; **po**, postorbital; **pof**, postfrontal; **pr**, prootic**; pra**, prearticular; **prf**, prefrontal; **ps**, parasphenoid; **pt**, pterygoid; **q**, quadrate; **so**, supraoccipital; **sq**, squamosal; **st**, supratemporal; **vo**, vomer. Scale bar equals 10 mm.

Keeble *et al.* 2018), the maxillary process bifurcates, but this secondary maxillary process is greatly reduced in size compared to the primary maxillary process and there is also very little space between the tooth-bearing region of the premaxilla and the point where the maxillary process bifurcates. *Clevosaurus convallis* (Säilä 2005) lacks this spur altogether. The premaxilla is robust and forms a brace for the snout, contacting the nasal at three points: (1) lateral surface of nasal process of premaxilla and medial surface of premaxillary process of nasal (Fig. 3A, B); (2) medial surface of primary maxillary process and lateral surface of nasal

(Fig. 3H); and (3) lateral surface of the secondary maxillary process and medial surface of nasal (Fig. 3A, H). It is questionable whether the premaxillae truly excluded the maxillae from the nares as in other *Clevosaurus*, as the maxillary facet covers the entire lateral surface of the dorsal process of the premaxilla.

Maxilla. The facial process of the maxilla (Fig. 3C–E) is very high and the premaxillary process is greatly reduced, similar to *C. bairdi* (Sues *et al.* 1994). Unlike *C. cambrica* and *C. bairdi* (Chambi-Trowell *et al.* 2019,
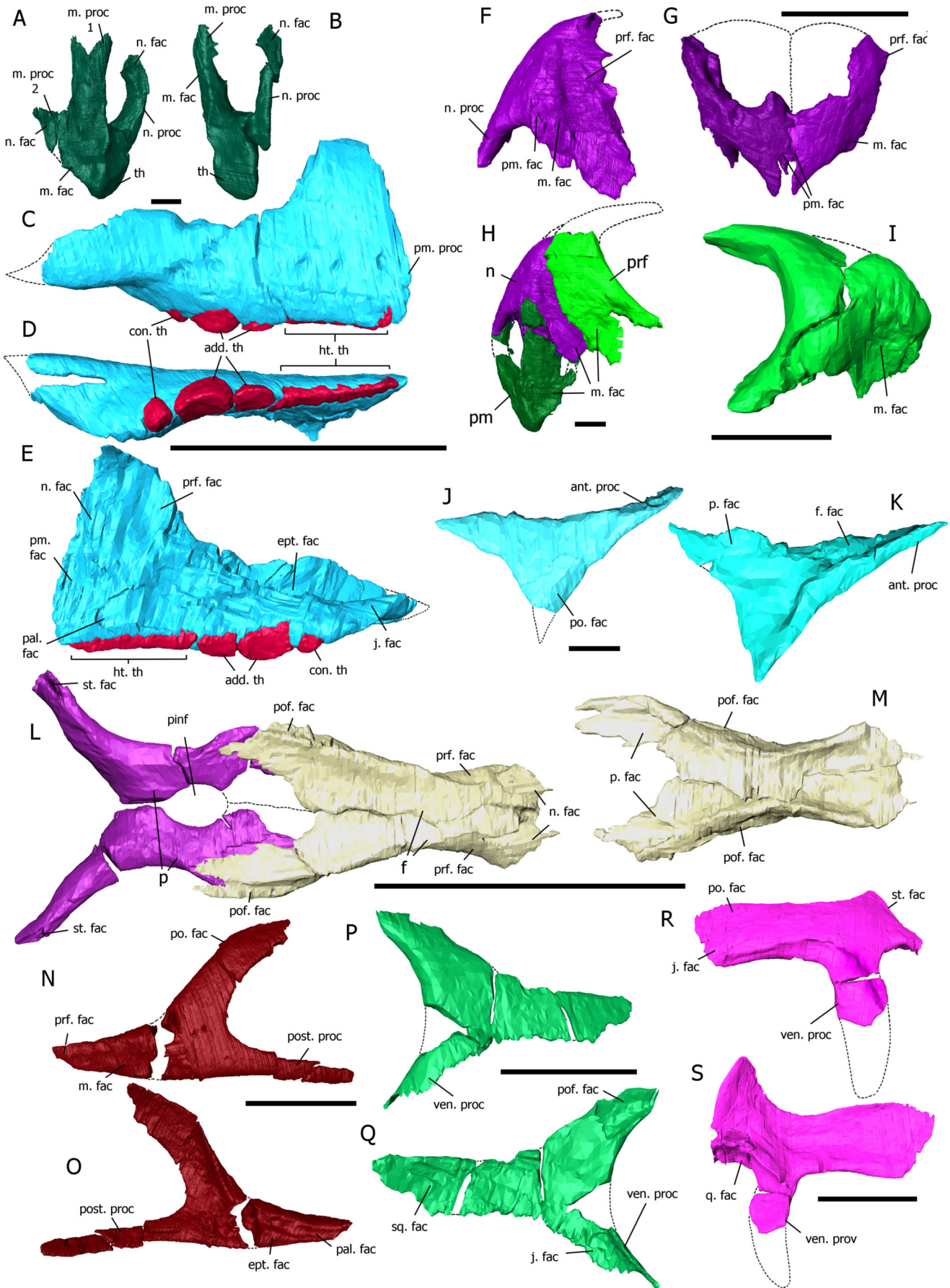
fig. 6B; Sues *et al*. 1994, fig. 1B), there is no posterior curvature of the maxillary dorsal process forming the sub- and antero-orbital margin (Fig. 3C). Posteriorly, the maxilla wraps around the jugal ventrally, but also bears facets for the premaxilla, nasal, prefrontal and ectopterygoids along its medial surface. Dorsally, the maxilla fits into a slot on the ventral edge of the anterior face of the descending process of the prefrontal so that the latter partially overlaps the maxilla both medially and laterally, forming a brace-like structure. The posterior process of the maxilla is broad, only tapering rapidly posteriorly beyond the end of the tooth row. The maxillary teeth are all deeply embedded in the bone, but do not possess true roots. This form of acrodonty (Fig. 4D–H, L, O) is not currently known in any other rhynchocephalian. Anteriorly, the maxilla possesses 12–13 small, presumably hatchling, teeth that are fused together and worn flat to the bone, most noticeably lingually (Fig. 3D, E), so that they form a sharp continuous cutting surface. Behind this 'beak' of hatchling teeth, *C. brasiliensis* typically bears two large, flanged teeth, a condition also seen in the other Norian clevosaur *Brachyrhinodon* and possibly also in *Polysphenodon* (Fraser & Benton 1989). The Early Jurassic *C. bairdi* (Sues *et al*. 1994) may have as few as three flanged teeth upon its maxilla, fewer than in clevosaurs from the UK and China. Most posteriorly, there are one or two smaller conical teeth, similar to *C. hudsoni* (Fraser 1988), but fewer than the three or four of *Microsphenodon* (see below).

Nasal. The nasals (Fig. 3F–H) are paired bones that are positioned nearly vertically and are much more convex than the nasals of *C. cambrica* (Chambi-Trowell *et al*. 2019) or *Microsphenodon* (see below), reflecting the steep short snout. Contrary to the original description (Bonaparte & Sues 2006) and the revision based on specimen MCN-PV 2852 (Hsiou *et al*. 2015), we find that the nasals are not fused with the frontals instead they interdigitate (Fig. 2D, Supplemental Fig. 4H). Anteriorly, they divide, forming an internarial slot where the nasal processes of the premaxillae could articulate. Laterally they bear a broad facet for the prefrontal, as

well as facets for the premaxilla and maxilla. Posteroventrally, there was a facet for the frontal.

Prefrontal. The prefrontal (Fig. 3H, I) forms the anterior half of the orbital margin, it is large and lunate in shape, and steeply curved where its anterodorsal process overlaps the frontal. The ventral process is expanded mediolaterally and forms a broad contact with the dorsal surface of the palatine (Fig. 2D) and would also have contacted the jugal. On the lateral surface of the prefrontal there is a broad partial slot facet forming a partial overlap of the top of the maxilla on both its medial and lateral sides.

Postfrontal. The postfrontal (Fig. 3J, K) is a small triradiate bone with a concave ventrolateral facet for the postorbital and a medially positioned concave facet that overlaps the parietal and frontal dorsally. It forms the posterodorsal margin of the orbit, and anterodorsal corner of the supratemporal fenestra. It is relatively larger than in other species such as *C. hudsoni* or *C. cambrica* (Keeble *et al*. 2018; O'Brien *et al*. 2018; Chambi-Trowell *et al*. 2019). In both UFRGS-PV-0748-T and UFSM-PV-0131 (Fig. 1A, D, 2A, D; Supplemental Fig. 2B, D) the anterior process of the postfrontal and posterior process of the prefrontal almost exclude the frontal from the orbital margin.

Frontal. When paired, the frontals (Fig. 3L, M) show the typical hourglass shape of *Clevosaurus*, and they are not fused, but interdigitate with one another along the medial axis. At the frontoparietal suture, the frontals diverge from one another posteriorly, forming two flattened processes that overlap the parietals. Anterolaterally, there is a step-like indentation indicating the prefrontal facet. The frontals contribute very little to the orbital margin.

Parietal. Articulating anterodorsally with the frontals, the parietals (Fig. 3L) are paired and not fused. Like other species of *Clevosaurus* (e.g. Fraser 1988, p. 174; Sues *et al*. 1994; Chambi-Trowell *et al*. 2019), they lack a parietal crest, differing from the condition seen in *Sphenodon*. Posteriorly the elongate posterior processes bear a distinct slot-like facet dorsally for the

Figure 3. Digital segmentation of selected cranial material of *Clevosaurus brasiliensis* (**A, B, F–H, R, S,** UFSM-PV-0131; **C–E, I–O,** UFRGS-PV-0748-T; **P, Q,** UFRGS-PV-0974-T). **A, B,** right premaxilla in **A,** lateral; and **B,** anterior views. **C–E,** right maxilla in **C,** lateral; **D,** ventral; and **E,** medial views. **F, G,** nasals in **F,** left lateral; and **G,** anterior views. **H,** rostrum in left lateral view. **I,** right prefrontal in lateral view. **J,** right postfrontal in lateral view. **K,** left postfrontal in medial view. **L,** parietals and frontals in dorsal view. **M,** frontals in ventral view. **N, O,** left jugal in **N,** lateral; and **O,** medial views. **P, Q,** left postorbital in **P,** lateral; and **Q,** medial views. **R, S,** left squamosal in **R,** lateral; and **S,** medial views. **Abbreviations: add,** additional; **ant,** anterior; **con,** conical; **ept,** ectopterygoid; **f,** frontal; **fac,** facet; **ht,** hatchling; **j,** jugal; **m,** maxilla; **n,** nasal; **p,** parietal; **pal,** palatine; **pinf,** pineal foramen; **pm,** premaxilla; **po,** postorbital; **pof,** postfrontal; **post,** posterior; **prf,** prefrontal; **proc,** process; **q,** quadrate; **sq,** squamosal; **st,** supratemporal; **th,** tooth; **ven,** ventral. Scale bars for C–E, L, M equal 10 mm; F, G, I, N–S equal 5 mm; and A, B, H, J, K equal 1 mm.
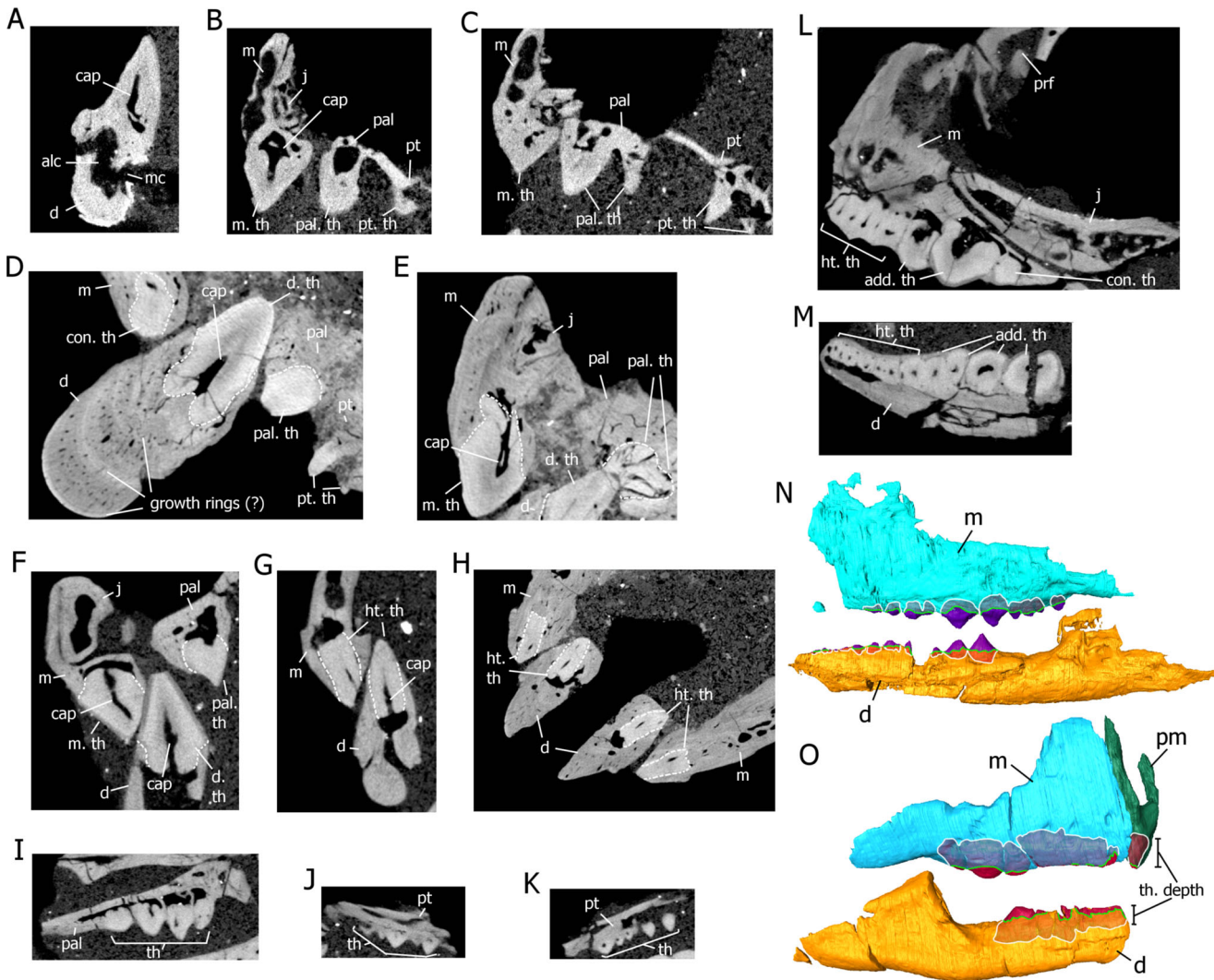
Figure 4. Cross-sections of the tooth implantation in *Microsphenodon bonapartei* gen. et sp. nov. (**A–C, N**) and *Clevosaurus brasiliensis* (**D–M, O**). **A–C,** coronal cross-sections showing tooth implantation in *Microsphenodon bonapartei* (UFRGS-PV-0972-T) in: **A,** posterior-most dentary tooth; **B,** posterior-most maxillary tooth; and **C,** palate. **D–H,** coronal cross-sections showing tooth implantation in *Clevosaurus brasiliensis* (UFRGS-PV-0748-T) in: **D,** posterior-most dentary tooth; **E,** penultimate additional maxillary tooth; and **H,** hatchling teeth; and for UFRGS-PV-0974-T in **F,** ultimate maxillary and dentary teeth; and **G,** hatchling teeth. Sagittal cross-sections of the bone bearing elements of *Clevosaurus brasiliensis* (UFRGS-PV-0974-T) for **I,** palatine; **J,** left pterygoid; **K,** right pterygoid; **L,** left maxilla; and **M,** left dentary. **N,** left maxilla and dentary of *Microsphenodon bonapartei* (UFRGS-PV-0972-T) demonstrating the depth of the acrodont implantation. **O,** left maxilla and dentary of *Clevosaurus brasiliensis* (UFRGS-PV-0748-T) demonstrating the depth of the acrodont implantation. **Abbreviations: add**, additional; **alc**, alveolar canal; **cap**, pulp cavity; **d**, dentary; **ht**, hatchling; **j**, jugal; **m**, maxilla; **mc**, Meckelian canal; **pal**, palatine; **pm**, premaxilla; **prf**, prefrontal; **pt**, pterygoid; **th**, tooth. Scale bars for A–K equal 1 mm; L–O equal 10 mm.

supratemporals and squamosal. The posterior processes are markedly more uniform in width and more elongate than those of *Microsphenodon* (see below).

Jugal. The jugals of UFRGS-PV-0748-T, UFSM-PV-0131 and UFRGS-PV-0974-T (Figs 1, 2; Supplemental Figs 1, 2) are relatively large and wide. The posterior process that forms the lower supratemporal bar is long, weakly contacting the quadrate and possibly forming a complete lower temporal bar (Supplemental Fig. 1B), as

previously proposed by Hsiou *et al.* (2015). The posterior process appears to be more ventrally deflected than that of the horizontal temporal bar of *Clevosaurus hudsoni* (Fraser 1988; O'Brien *et al.* 2018) or *Sphenodon*, and more like that of *Brachyrhinodon* (Fraser & Benton 1989). The anterior process of the jugal reaches the anterior orbital margin, where it contacts the prefrontal (Figs 1D, 3D), and has a broad contact with the ectopterygoid medially and slots into the medially curved posterior process of the maxilla. The anterior process
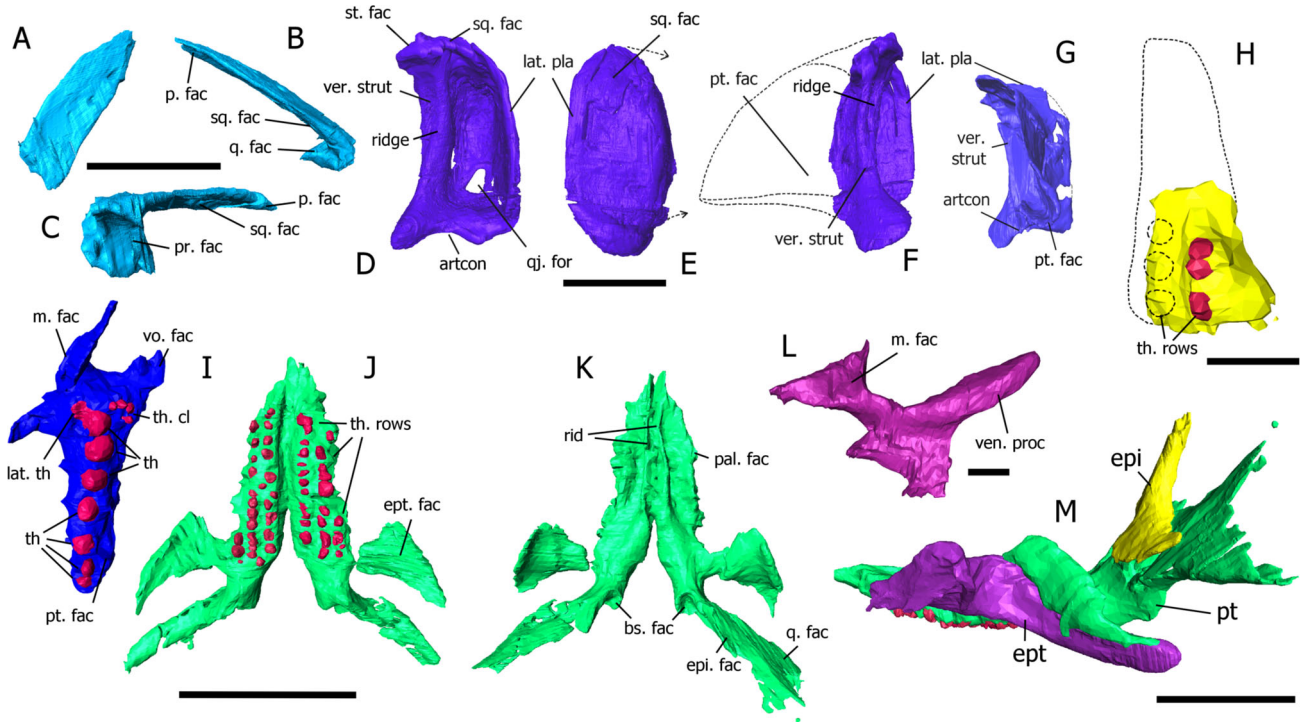
Figure 5. Cranial material of *Clevosaurus brasiliensis* (**A–F,** UFSM-PV-0131; **G–M,** UFRGS-PV-0748-T). **A–C,** left supratemporal in: **A,** posterolateral; **B,** anteromedial; and **C,** posteroventral views. **D–F,** right quadrate in: **D,** posterior; **E,** lateral; **F,** medial views. **G,** left quadrate in anteromedial view. **H,** left vomer in ventral view. **I,** right palatine in ventral view. **J, K,** pterygoids in **J,** ventral; and **K,** dorsal views. **L,** left ectopterygoid in ventral view. **M,** palate in left lateral view. **Abbreviations: artcon**, articular condyle; **bs**, basisphenoid; **cl**, cluster; **epi**, epipterygoid; **ept**, ectopterygoid; **fac**, facet; **for**, foramen; **lat**, lateral; **m**, maxilla; **p**, parietal; **pal**, palatine; **pla**, plate; **pr**, prootic; **pt**, pterygoid; **q**, quadrate; **qj**, quadratojugal; **rid**, ridge; **sq**, squamosal; **st**, supratemporal; **th**, tooth; **ven**, ventral; **ver**, vertical; **vo**, vomer. Scale bars for A–G, I–K, M equal 5 mm; H, L equal 1 mm.

may also have contacted the maxillary process of the palatine anteriorly. The dorsal process contacts the post-orbital, with an interdigitating suture rather than simple overlapping facets as in *C. hudsoni* or *C. cambrica* (Fraser 1988; Chambi-Trowell *et al*. 2019). Posterodorsally, the dorsal process overlaps the squamo-sal. Overall, the jugals are more robust than in European *Clevosaurus* (Fraser 1988; Klein *et al*. 2015) and similar to those of *C. bairdi* (Sues *et al*. 1994).

Postorbital. A large triradiate bone, the postorbital (Fig. 3P, Q) is similar in size to that of *C. bairdi* (Sues *et al*. 1994), though relatively smaller and with a shorter ven-tral process, unlike other *Clevosaurus*, such as *C. cambrica* and *C. hudsoni* (Fraser 1988; Chambi-Trowell *et al*. 2019). Uniquely for Rhynchocephalia, the post-orbital does not overlap the dorsal process of the jugal but rather interdigitates with it along its ventral edge. Posteriorly, it has a broad facet that overlies the squamosal. The dorsal process is large and contacts the postfrontal ventrally, partially wrapping around its anter-ior margin.

Squamosal. The ventral process of the squamosal (Fig. 3R, S) is broad and curved, forming a broad contact with the quadrate. The anterior flange is large and artic-ulates dorsally with the postorbital and jugal. The medi-ally curved posterior process articulates with the supratemporal on its posterolateral surface. The medial surface is, for the most part, smooth and concave, but dorsal to the ventral process the squamosal widens medially, forming a robust cup-like structure (Fig. 3S) that articulates with the dorsal condyle of the quadrate. On the lateral surface there is a depression that starts from the anteroventral-most point of the squamosal and initially runs posterodorsally at a shallow angle, before curving ventrally with the ventral process and terminat-ing half-way down the posterior margin of the ven-tral process.

Supratemporal. The supratemporal (Fig. 5A–C) is a convex plate-like bone that connects the squamosal to the parietal along its medial surface and forms the pos-terior margin of the supratemporal fenestra. Midway along its long axis there is a parallel indentation, pos-sibly marking the origin of the M. depressor mandibulae

that inserted on the remarkably long retroarticular process. The supratemporal is roughly rectangular in shape, similar to that of other *Clevosaurus* (Fraser 1988; Sues *et al.* 1994; Jones 2006) and *Microsphenodon*. Posteriorly, the supratemporal curves anteriorly, forming a hook that would have articulated with the posterior edge of the dorsal condyle of the quadrate. On the posterior surface of this hook, the supratemporal articulated with the paroccipital process.

Quadrate. The quadratojugal cannot be distinguished from the quadrate. Anteriorly, the thin quadrate flange tapers to a point. The quadrate (Fig. 5D–G) is a complex element, forming a thin lateral plate posterolaterally, with a raised, reinforced posterior margin, and posteromedially a robust strut (Fig. 5D, F) between the cephalic and articular condyles. The ventral process of the squamosal articulated to the quadrate anterior to the raised margin of the lateral plate, while most of the squamosal articulated on the cephalic condyle of the quadrate. The vertical strut and lateral plate contact one another dorsally and ventrally, forming a conch-like structure that is concave anteriorly, and with a quadratojugal foramen present anterolaterally. The quadrate flange is reinforced along its ventral margin where it curves, forming a raised rim into which the flange of the pterygoid slotted (Fig. 5G). The bone is spongy around both cephalic and articular condyles. The vertical strut is much more robust than observed in other *Clevosaurus* (Fraser 1988; Chambi-Trowell *et al.* 2019, fig. 2D, E), and this strut twists so that a raised ridge (Fig. 5F) begins on the lateral side towards the dorsal end of the quadrate and ends up contacting the medial side ventrally.

Vomer. No complete vomers are known, but a fragment of the left vomer is preserved still articulated dorsally to the anterior of the palatine and pterygoid in both UFRGS-PV-0748-T (Fig. 5H) and UFRGS-PV-0974-T. Known vomer fragments bear two rows of small teeth, with three small medial row teeth on a raised bony ridge, and a lateral row with another three teeth in MCN-PV 2852 (Hsiou *et al.* 2015). Although represented by just fragments, it is clear there are more teeth on the vomer of *C. brasiliensis* than in *C. hudsoni* or *C. cambrica* (Fraser 1988; Chambi-Trowell *et al.* 2019).

Palatine. The palatines (Figs 4I, 5I, 6A–D) differ from the roughly triangular bones present in other *Clevosaurus* (Fraser 1988; Jones 2006; Klein *et al.* 2015; Chambi-Trowell *et al.* 2019) as well as basal rhynchocephalians such as *Gephyrosaurus*, *Planocephalosaurus* and *Diphydontosaurus* (Evans 1980; Fraser 1982; Whiteside 1986), or even non-rhynchocephalians such as *Kuehneosaurus* (Robinson 1962).

The *Clevosaurus brasiliensis* palatines are more similar in shape to those of *Sphenotitan*, being very narrow and widening abruptly anteriorly where they bear a medial cluster of smaller teeth. However, *Sphenotitan* has 12 to 13 teeth in the lateral row whereas *C. brasiliensis* has five to seven. The palatines are elongate and narrow, forming an elevated ridge that interdigitates along the medial side with the anterior pterygoid process and widens abruptly, but not extensively, anterior to the pterygoid. The palatine bears the typical lateral row of large teeth, five to seven in a row, as in many *Clevosaurus* species (Fraser 1988; Säilä 2005; Jones 2006; Klein *et al.* 2015; Chambi-Trowell *et al.* 2019) and *Microsphenodon*, but more than the four in *C. minor* (Fraser 1988). There is a cluster of four to six small, medially positioned teeth in the same anterior region as the large singular medially placed tooth that is found in all other *Clevosaurus*; one palatine of *C. hudsoni* (AUP 11158; Fraser 1988, p. 137) is thought to have had a rudimentary second row of three teeth in the position of this singular tooth. Anterolaterally to the main tooth row, there is sometimes a single small, mesiodistally elongate tooth (Fig. 6B) that is fused to the lateral edge of the anterior-most tooth of the lateral row (clearly visible in UFRGS-PV-0748-T and UFRGS-PV-0974-T), forming a two-cusped tooth that is unlike anything seen in any other rhynchocephalian. The robust maxillary process bifurcates to form a very broad contact with the maxilla, possibly even reaching the premaxilla; posteriorly this process contacts the jugal, isolating the maxilla from the orbit medially. Posteriorly, the palatine ventrally overlaps the ectopterygoid. Similar to other species of *Clevosaurus* (cf. *C. minor*; Fraser 1988, pp. 159–160), it possesses a concave vomerine facet. Dorsally, the prefrontal articulates with the anterior edge of the palatine. Unlike the curved lateral tooth row of the Chinese clevosaurs (Wu 1994; Jones 2006, fig. 1B), the row of palatine teeth can be almost completely straight or even medially concave (Wu 1994; Jones 2006).

Pterygoid. Uniquely among *Clevosaurus* species, but like more basal sphenodontians such as *Planocephalosaurus* (Fraser 1982), the pterygoids (Fig. 5J–M) bear three rows of teeth. The lateral-most row is the shortest, with just three teeth, the same as *Microsphenodon*, whereas there are only two teeth in the possibly contemporary clevosaur *Brachyrhinodon* (SAVC-T, pers. obs.) and in *Planocephalosaurus*. There is some alternation in the size of teeth on both the pterygoids of UFRGS-PV-0974-T (Fig. 4J, K). As in *Clevosaurus cambrica* and *Clevosaurus hudsoni* (Fraser 1988, pp. 137–138; Chambi-Trowell *et al.* 2019), the ramus that runs between the tooth-bearing region of the
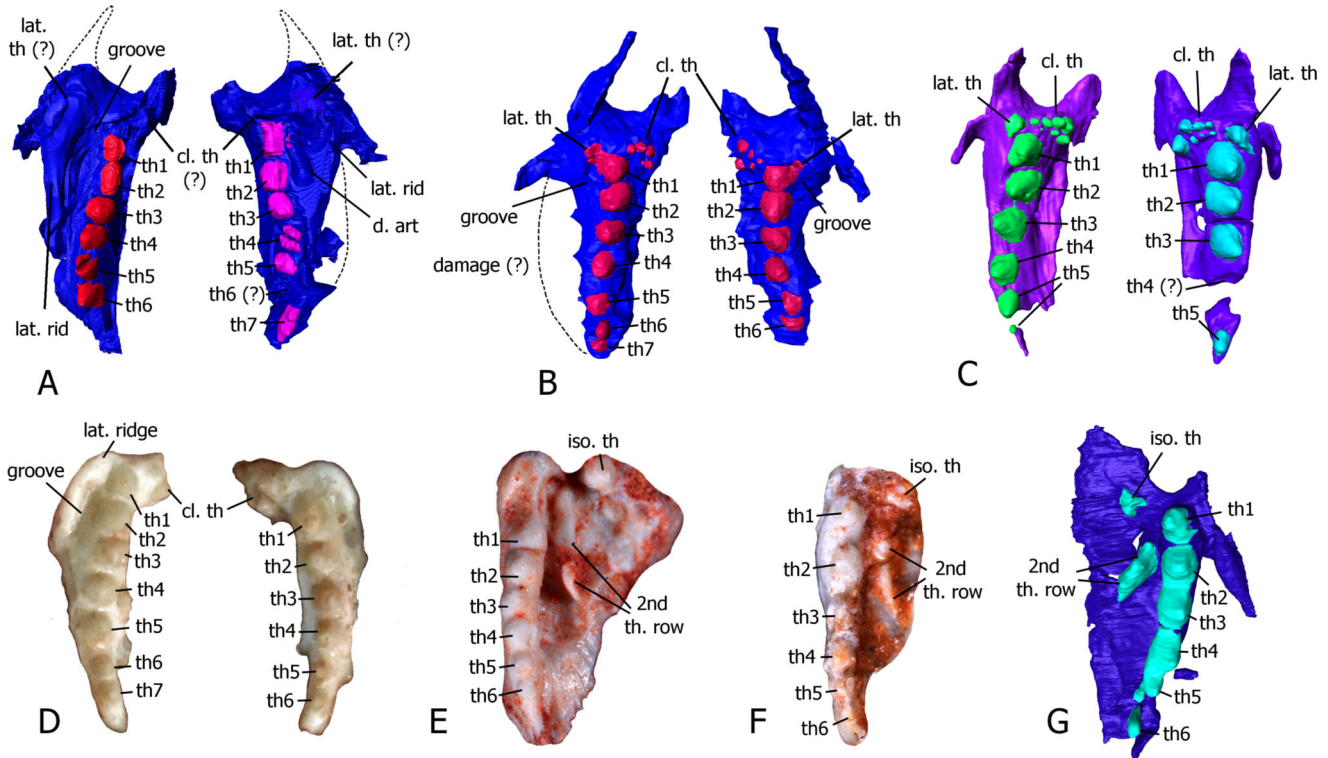
Figure 6. Ventral view of palatines for *Clevosaurus brasiliensis* (**A–D**), and *Microsphenodon bonapartei* gen. et sp. nov. (**E–G**). **A,** UFSM-PV-0131; **B,** UFRGS-PV-0748-T; **C,** UFRGS-PV-0974-T; **D,** MCN-PV 2852. **E,** right palatine, UFRGS-PV-0827-T; **F,** right palatine, UFRGS-PV-0613-T; **G,** left palatine, UFRGS-PV-0972-T. **Abbreviations: cl**, cluster; **d**, dentary; **iso**, isolated; **lat**, lateral; **rid**, ridge; **th**, tooth. Not to scale.

pterygoid and the articulation point for the basipterygoid processes is relatively short compared to *Sphenodon*. The pterygoid flange articulates medially with the quadrate flange, which partially wraps around its ventral margin. The pterygoid lateral processes that articulate ventrally with the ectopterygoids appear typical of *Clevosaurus*, the processes being roughly triangular in shape with an elongated posterior end. Posteriorly, the pterygoid bends sharply as the pterygoid flanges extend posterolaterally, and there is a posteriorly positioned rounded facet for the basipterygoid process. About halfway along the flange is a small dorsally positioned spike (Fig. 5K, M) where the epipterygoid articulates. The two pterygoids articulate anteriorly with an interdigitated facet, and there is a pronounced ridge of bone on either side of this facet on the dorsal surfaces of the pterygoids.

Ectopterygoid. The ectopterygoid (Fig. 5L, M) appears typical of *Clevosaurus*. Anteriorly, its lateral process contacts the palatine lateral process, which has a broad contact laterally with the maxilla and jugal, as in *C. bairdi* (Sues *et al*. 1994) and *C. cambrica* (Chambi-Trowell *et al*. 2019). Medioanteriorly on its ventral side it bears a facet for the palatine, and medioposteriorly it

articulates with the pterygoid. Its posterior lateral process is roughly triangular and articulates with a similar process on the pterygoid.

Epipterygoid. The epipterygoid (Fig. 5M) is tall and columnar, rod-like dorsally and flattening and broadening ventrally to its articulation with the pterygoid flange, as in *C. cambrica* (Chambi-Trowell *et al*. 2019, fig. 8C), *C. bairdi* (Sues *et al*. 1994) and *Microsphenodon*. This shape differs markedly from *C. hudsoni* NHMUK PV R36832 (O'Brien *et al*. 2018), which suggests that the epipterygoid described there, although somewhat reminiscent of the epipterygoid of *Sphenodon*, might be the broken displaced right paroccipital process.

Parabasisphenoid. The parasphenoid and basisphenoid are fused (Fig. 7A–E), as in other species of *Clevosaurus* (Fraser 1988, fig. 18; Hsiou *et al*. 2015; Chambi-Trowell *et al*. 2019), forming the floor of the braincase and widening posteriorly. Anteriorly, there are two elongate basipterygoid processes that articulate with the pterygoids. The cultriform process has broken off in the specimens that we examined, but in MCN-PV 2852 (Hsiou *et al*. 2015) it is seen to be thin and elongate.
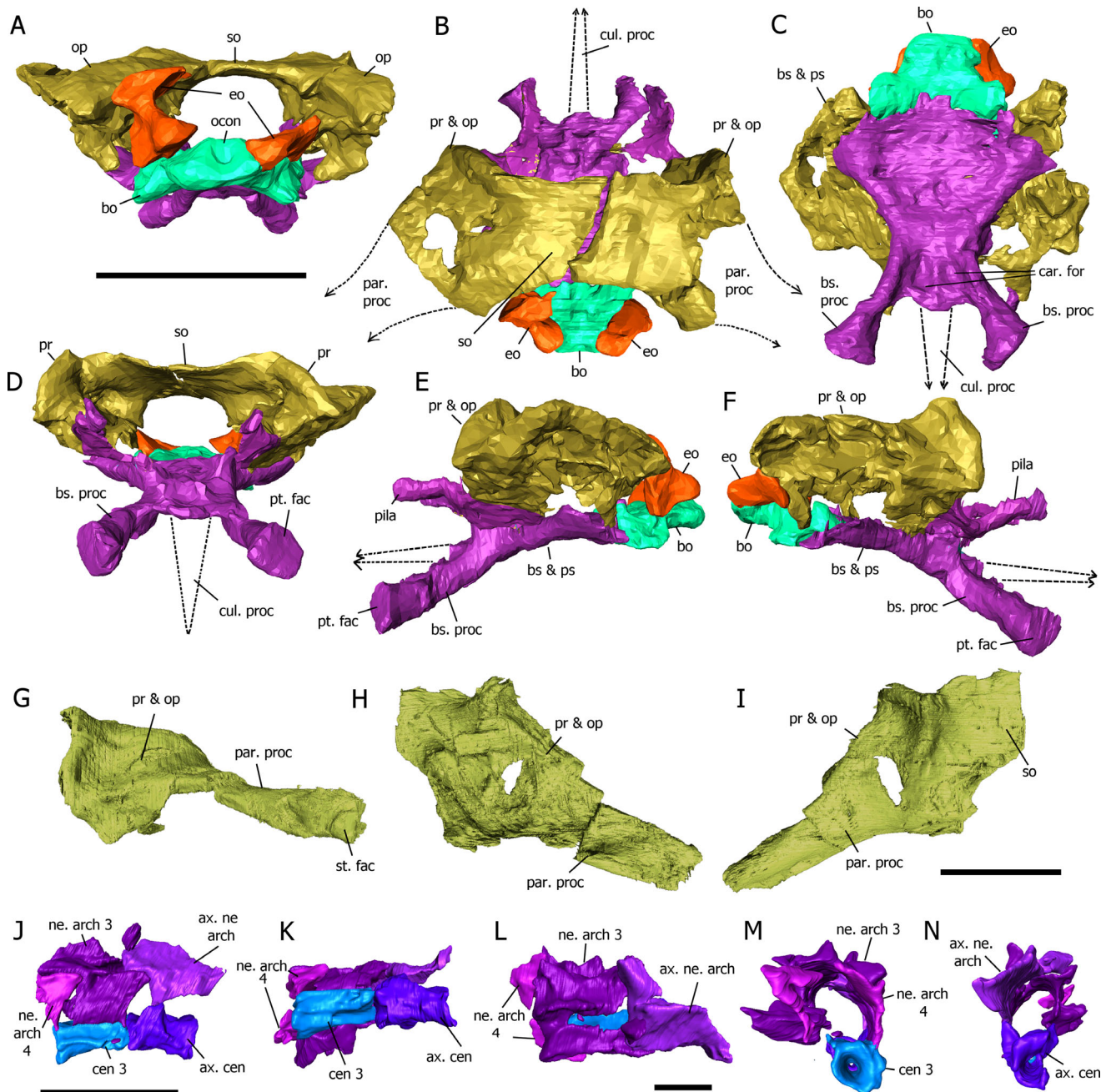
Figure 7. The braincase and cervical vertebra of *Clevosaurus brasiliensis* (**A–F,** UFRGS-PV-0748-T; **G–I,** UFSM-PV-0131; **J–N,** UFRGS-PV-0974-T). **A–F,** near-complete braincase of UFRGS-PV-0748-T in: **A,** posterior; **B,** dorsal; **C,** ventral; **D,** anterior; **E,** left lateral; and **F,** right lateral views. **G–I,** the partial left half of the braincase of UFSM-PV-0131 in: **G,** anterolateral; **H,** ventral; and **I,** dorsal views. **J–N,** the articulated cervical vertebra of UFRGS-PV-0974-T in: **J,** right lateral; **K,** ventral; **L,** dorsal; **M,** posterior; and **N,** anterior views. **Abbreviations: ax**, axis; **bo**, basioccipital; **bs**, basisphenoid; **car. for**, carotid foramen; **cen**, centrum; **cul. proc**, cultriform process; **eo**, exoccipital; **fac**, facet; **ne. arch**, neural arch; **ocon**, occipital condyle; **op**, opisthotic; **par**, paroccipital; **pila**, pila antotica; **pr**, prootic; **proc**, process; **ps**, parasphenoid; **pt**, pterygoid; **so**, supraoccipital; **st**, supratemporal. Scale bar for A–L equals 5 mm; M, N equals 1 mm.

Basioccipital. The basioccipital (Fig. 7A–E) is similar to that of other species of *Clevosaurus*, with a lunate occipital condyle and two robust basal tubera, but these project laterally and are very short, more similar to *Planocephalosaurus* (Fraser 1982) than posterolaterally as in *C. cambrica*, *C. hudsoni* and *C. sectumsemper* (Fraser 1988; Klein *et al.* 2015; O'Brien *et al.* 2018; Chambi-Trowell *et al.* 2019). It articulates
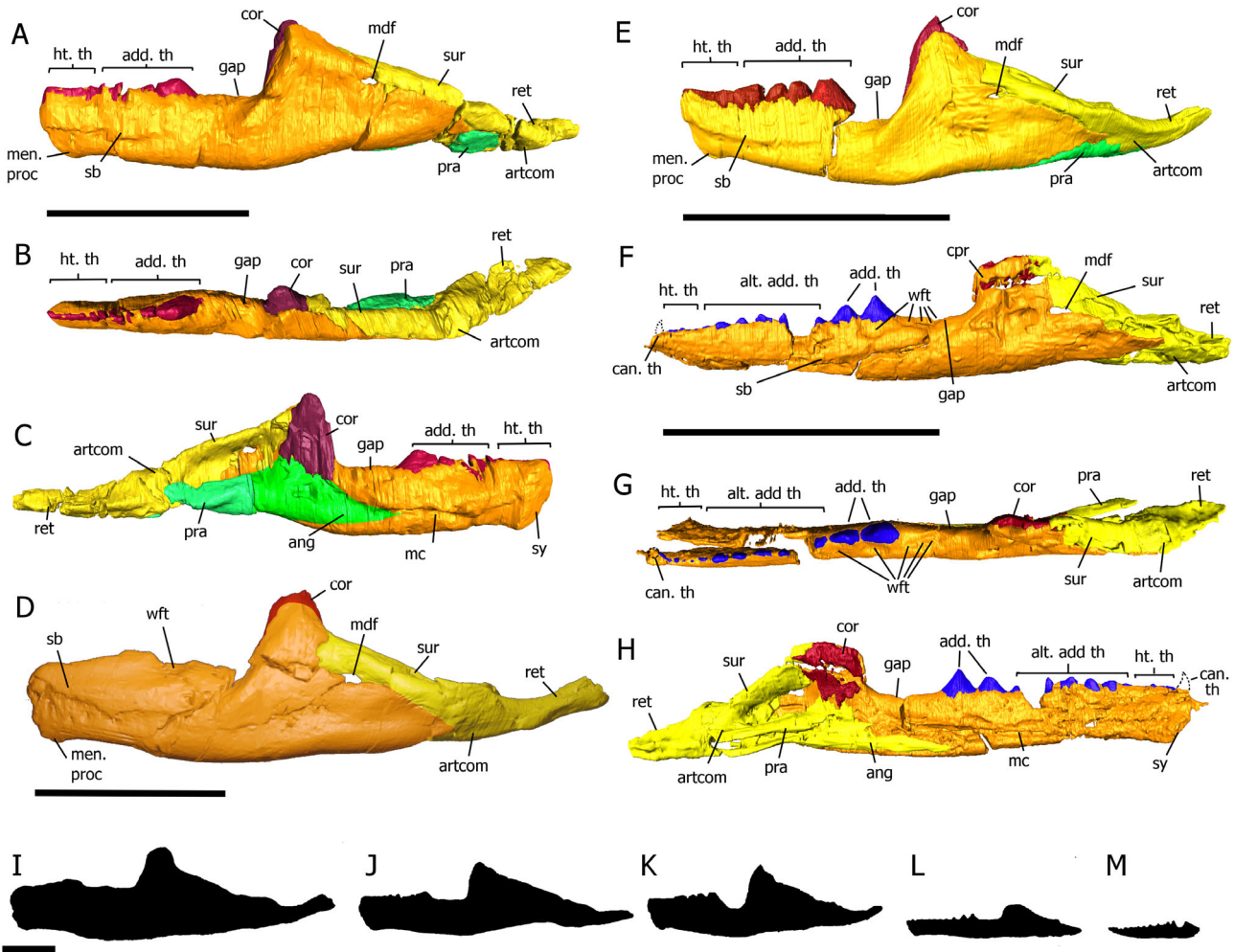
Figure 8. The lower left mandible of Brazilian sphenodontians. **A–C, J,** *Clevosaurus brasiliensis* (UFRGS-PV-0748-T) in: **A,** lateral; **B,** dorsal; **C,** medial; and **J,** scaled lateral views. **D, I,** *Clevosaurus brasiliensis* (UFSM-PV-0131) in: **D,** lateral; and **I,** scaled lateral views. **E, K,** *Clevosaurus brasiliensis* (UFRGS-PV-0974-T) in: **E,** lateral; and **K,** scaled lateral views. **F–H, L,** *Microsphenodon bonapartei* gen. et sp. nov. (UFRGS-PV-0972-T) in: **F,** lateral; **G,** dorsal; **H,** medial; and **L,** scaled lateral views. **M,** *Lanceirosphenodon* (CAPPA/UFSM 0226) in scaled view. **Abbreviations: add**, additional; **alt**, alternating; **ang**, angular; **artcom**, articular complex; **cor**, coronoid; **cpr**, coronoid process; **ht**, hatchling; **mc**, Meckelian canal; **men**, mentonian; **mdf**, mandibular foramen; **pra**, prearticular; **proc**, process; **ret**, retroarticular; **sb**, secondary bone; **sur**, surangular; **sy**, symphysis; **th**, tooth; **wft**, wear facet. Scale bars equal 10 mm.

anteroventrally with the parabasisphenoid and bears anteroposteriorly elongated grooves anteriorly of the basal tubera (Fig. 7A, E), where the exoccipitals would have articulated dorsally.

Exoccipitals. Dorsally, the exoccipitals (Fig. 7A–E) are broad and rounded, tapering rapidly towards the supraoccipital, and would have formed more than 50% of the foramen magnum, including the lateral margin, as well as a portion of the ventral and dorsal margins. Ventrally, they articulate with the basioccipital and anterodorsally with the opisthotic. Unlike the condition in basal rhynchocephalians such as *Gephyrosaurus*, *Planocephalosaurus* and *Diphydontosaurus* (Evans

1980; Fraser 1982; Whiteside 1986), as well as *Microsphenodon*, the exoccipitals are not fused to the basioccipital, a feature in common with other species of *Clevosaurus* (Fraser 1988; Klein *et al.* 2015; Chambi-Trowell *et al.* 2019).

Opisthotics, prootics and supraoccipital. The roof of the skull is formed from the opisthotics, prootics and supraoccipital (Fig. 7A–I). All three appear fused and are not individually distinguishable, as also in *C. hudsoni* and *C. cambrica* (Fraser 1988, p. 140; Chambi-Trowell *et al.* 2019). The bones here appear to have a lower bone density than the rest of the skull, and as a result it is hard to distinguish them from the matrix. The

supraoccipital forms part of the dorsal margin of the foramen magnum, and its dorsal surface is broad and concave with no dorsal crest. The pila antotica appears typical for *Clevosaurus* but also broken on both sides so that it would likely have stood more upright in life. The prootic bears a large concave facet posteriorly for the exoccipital. The paroccipital processes are elongate and articulate with the supratemporals.

Mandible.

Dentary. The dentary (Fig. 8A–E, I–K) shows a pronounced gap between the ultimate tooth and the coronoid process, which may be concave in lateral profile, as is generally the case in clevosaurs, except in some specimens of *C. convallis* (Säilä 2005). The coronoid process is markedly high, and the dentary is the most robust of all *Clevosaurus*, although it is also sturdy in *C. convallis* (Säilä 2005) and *C. bairdi* (Sues *et al.* 1994). In cross-section, the dentary of the holotype was observed to have three possible growth rings (Fig. 4D), indicating three cycles of growth, though it is uncertain whether these correspond with years. The symphysis is near vertical and robust, and lacks any concavity medially (Fig. 8C), differing from European clevosaurs such as *C. sectumsemper* and *C. cambrica* (Klein *et al.* 2015, fig. 4; Chambi-Trowell *et al.* 2019). The mentonian process is reduced but rounded and robust (Fig. 8D).

The dentary bears 12–13 teeth in total, the ultimate additional tooth is huge (two to three times larger than any of the other teeth) and is mesiodistally elongated. Most anteriorly, there are eight to 10 teeth that become gradually smaller anteriorly and are considered here to be hatchling teeth. These are fused together (Fig. 4M) and are worn flat to the dentary, with the lateral edge of the bone worn away to expose their long 'roots' (Fig. 4G, H, O), thereby forming a continuous cutting surface like a beak. Posteriorly, there are three to four additional teeth, each circular in cross-section, except for the large mesiodistally elongated posterior-most tooth. In some specimens, there can be as few as two additional teeth (UFRGS-PV-1153-T; Romo de Vivar Martínez & Soares 2015).

The tooth-bearing region of the dentary is reduced relative to the length of the entire mandible and lacks the diagonal wear facets seen on the dentaries of the UK *Clevosaurus* (Fraser 1988; Klein *et al.* 2015; Chambi-Trowell *et al.* 2019). The wear facets of *C. brasiliensis* are smooth and form a continuous secondary ridge above the secondary dentine (Fig. 8D), possibly similar to those of *C. mcgilli* (Jones 2006). There is a pronounced lip of secondary bone along the lateral surface of the dentary, as in many rhynchocephalians. *Clevosaurus brasiliensis* lacks the characteristic saddle-shaped additional dentary teeth of most European *Clevosaurus* (Fraser 1988; Klein *et al.* 2015; Chambi-Trowell *et al.* 2019) and bears triangular teeth which are heavily worn dorsally. There are no flanges on the dentary teeth, and they lack noticeable escape structures. The teeth of *C. brasiliensis* are acrodont but are deeply imbedded within the jaws, up to half the depth of the dentary in places (Fig. 4D, G, O), a condition not seen in any other rhynchocephalian. The teeth do not have true roots or sockets, but rather they are packed together in a long groove, many showing fusion to the next tooth, with bone surrounding them both labially and lingually. We suggest that this condition might have developed by growth of secondary bone over the bases of the teeth to such an extent that the teeth are nearly obscured with secondary bone. This is further supported by the condition in UFRGS-PV-0974-T, which we infer to be the youngest of the three specimens because its teeth are noticeably less worn than the others, where the deep acrodont implantation of the teeth is more pronounced than the posterior-most teeth (Fig. 4F).

Coronoid. The coronoid (Fig. 8A–E) is a simple inverted tear drop-shaped bone that is laterally flattened, tapering ventrally. Similar to *C. bairdi*, *C. cambrica* and *C. hudsoni* (Sues *et al.* 1994; Chambi-Trowell *et al.* 2019) it projects slightly above the coronoid process. It is articulated laterally to the dentary and posteriorly to the surangular. In some specimens (UFSM-PV-0131, UFRGS-PV-0974-T; Fig. 8D, E) the coronoid projects above the dentary, and appears to curve backwards as in *Sphenodon* and many squamates.

Articular complex (prearticular, surangular, articular and angular). The prearticular and articular are not fused (Fig. 8A–E), unlike in most *C. hudsoni*, *C. cambrica* and *C. convallis* specimens (Fraser 1988; Säilä 2005; Chambi-Trowell *et al.* 2019), though a lack of fusion has been observed in some individuals of *C. hudsoni* (Fraser 1988, p. 141). The prearticular is a long, flattened bone that wraps medially beneath the articular, and laterally contacts the dentary; it becomes more rounded and complex in shape anteriorly, forming

---

Figure 9. Cranial material of *Microsphenodon bonapartei* gen. et sp. nov. (**A,** UFRGS-PV-0972-T; **B, C,** UFRGS-PV-0613-T; **D, E,** UFRGS-PV-0827-T; **F,** UFRGS-PV-0848-T). **A,** left lateral view of the holotype near-complete skull UFRGS-PV-0972-T. **B, C,** partial skull of UFRGS-PV-0613-T in: **B,** left lateral; and **C,** ventral views. **D, E,** right palatine UFRGS-PV-0827-T in: **D,** right lateral; and **E,** ventral views. **F,** medial view of left dentary UFRGS-PV-0848-T. Scale bars equal 5 mm.
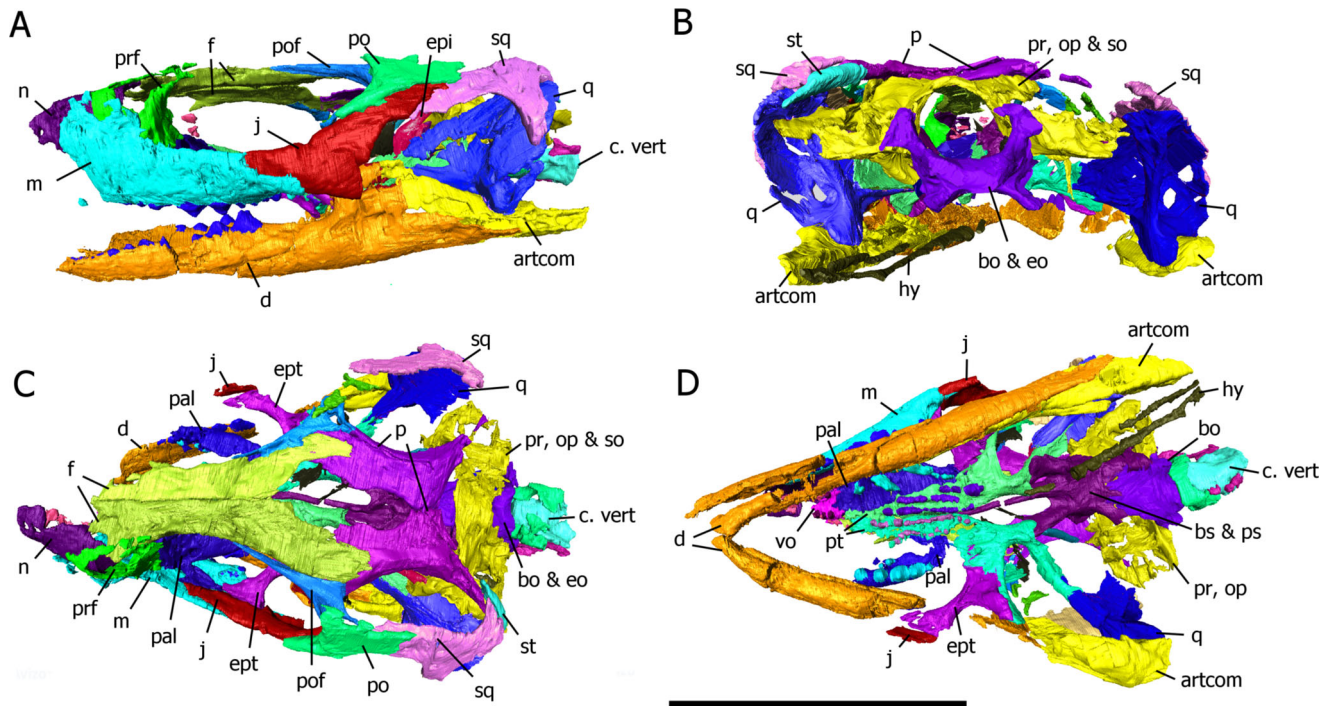
Figure 10. The digitally segmented holotype skull of *Microsphenodon bonapartei* gen. et sp. nov. (UFRGS-PV-0972-T). **A,** left lateral; **B,** posterior; **C,** dorsal; and **D,** ventral views. **Abbreviations: artcom**, articular complex; **bo**, basioccipital; **bs**, basisphenoid; **c. vert**, cervical vertebra; **d**, dentary; **eo**, exoccipital; **epi**, epipterygoid; **ept**, ectopterygoid; **f**, frontal; **hy**, hyoid; **j**, jugal; **m**, maxilla; **n**, nasal; **op**, opisthotic; **p**, parietal; **pal**, palatine; **po**, postorbital; **pof**, postfrontal; **pr**, prootic; **prf**, prefrontal; **ps**, parasphenoid; **pt**, pterygoid; **q**, quadrate; **so**, supraoccipital; **sq**, squamosal; **st**, supratemporal; **vo**, vomer. Scale bar equals 10 mm.

the lower bar of the adductor fossa. The surangular and articular are fused, as in other species of *Clevosaurus* (Fraser 1988; Chambi-Trowell *et al*. 2019). The surangular process is moderately curved so that its dorsal surface is somewhat convex, articulating anteriorly with the posterior surface of the coronoid. The articular is a long, flattened bone that posteriorly contacts the prearticular, and tapers anteriorly, terminating below the posterior-most tooth. The dorsal surface of the surangular is also very broad mediolaterally and robust compared to other rhynchocephalians. The articular is robust with a remarkably long retroarticular process that forms a spoon-like structure that tapers posteriorly and is deepest laterally. The small mandibular foramen is formed between the surangular and dentary. The condyle is full of spongy bone.

Postcranial skeleton. Little postcranial material (Fig. 7J–N) is preserved in the specimens we examined. However, there are a few cervical vertebrae that had been dislocated from the skull in UFRGS-PV-0974-T, including a probable axis, but with the damage they have sustained dorsally, it is not possible to verify the position in the neck. UFRGS-PV-0974-T also appears to have fragments of a long bone, likely the humerus.

Lepidosauria Haeckel, 1866 [*sensu* de Queiroz & Gauthier 2020]
Rhynchocephalia Günther, 1867 (*sensu* Gauthier, Estes & de Queiroz 1988)
Sphenodontia Williston, 1925 (*sensu* Benton 1985)
Eusphenodontia Herrera-Flores, Stubbs, Elsler & Benton, 2018
Microsphenodon gen. nov.

Type and only known species. *Microsphenodon bonapartei* sp. nov.

Derivation of name. 'Micro' is derived from the Greek μικρό (mikró) which means small, and '*Sphenodon*' refers to the sole extant genus of rhynchocephalian. Like *Sphenodon*, the animal has caniniforms and pronounced differentiation of its teeth, but is itself a much smaller animal, therefore 'small *Sphenodon*'.

Microsphenodon bonapartei sp. nov.
(Figs 4, 6, 8–14; Supplemental Fig. 4)

Holotype. UFRGS-PV-0972-T (Fig. 9A, 10), a near-complete skull with some damage to its rostrum and missing the premaxillae and vomers. Much of the right

side of the skull is damaged, but only the right maxilla and jugal are entirely missing. For the most part, the skull remains articulated and would have been ~19 mm in length.

Derivation of name. The specific term '*bonapartei*' refers to the late Argentinian palaeontologist José F. Bonaparte (1928–2020), who led the main collections of fossil vertebrates from the Linha São Luis outcrop until 2005, deposited at the UFRGS, including the discovery of the holotype specimen here described.

Additional referred specimens. UFRGS-PV-0613-T, UFRGS-PV-0848-T and UFRGS-PV-0827-T are referred to the new taxon, which were identified as *C. brasiliensis* in previous studies (Bonaparte & Sues 2006; Romo de Vivar Martínez & Soares 2015; Romo-de-Vivar-Martínez *et al.* 2021). UFRGS-PV-0613-T is a partial skull around 20 mm long, and is in similar condition to the holotype, with damage to its rostrum and the right side of the skull; it was described by Bonaparte & Sues (2006) as the paratype of *C. brasiliensis*, where they interpreted it to be a juvenile of the taxon. UFRGS-PV-0848-T is an isolated right mandible 24 mm long. UFRGS-PV-0827-T is an isolated right palatine.

Diagnosis. A small sphenodontian rhynchocephalian with a skull length of 19–22 mm, which has the following unique combination of features:
1. A single caniniform tooth present on both maxilla and dentary.
2. The maxillary and dentary dentition is acrodont and the largest teeth take the form of two enlarged mesiodistally elongated additional teeth at the posterior of the dentary and maxilla, posterior to a row of smaller non-hatchling teeth that alternate in size.
3. A broad flat parietal table.
4. Three to four small conical post-marginal teeth positioned behind the additional teeth of the maxilla.
5. A palatine with a single medially positioned tooth, in addition to a secondary row or ridge of two teeth that are positioned at 45° to the long axes of the main lateral tooth row.
6. Fused prearticular, articular and surangular bones.
7. Paired frontals and parietals.
8. Exoccipitals fused to basioccipital.
9. Two rows of vomerine teeth, three rows of pterygoidal teeth and two rows of palatine teeth.

Description
Skull. Nearly all bones of the skull are represented, but there is no complete vomer, any premaxillae or verifiable stapes.

Maxilla. The maxillary facial process (Fig. 11A–C) is relatively high but not as much as in *Clevosaurus brasiliensis* and is broader. It bears a pronounced premaxillary process and a single caniniform (UFRGS-PV-0613-T, Romo de Vivar Martínez & Soares 2015, fig. 3C, 4F; Fig. 9B, C), which is followed by an edentulous region where the likely hatchling teeth have been worn to the bone, followed by around three to four smaller additional teeth that appear to alternate in size (Romo de Vivar Martínez & Soares 2015, fig. 4F), and ultimately two large additional teeth bearing flanges. All the teeth are acrodont (Fig. 4A–C, N). Posterior to the main tooth row are three to four small conical teeth. It is unclear whether the premaxillary process bore any successional teeth anterior to the caniniform, as this part of the maxilla is damaged. The posterior process is broad and only narrows abruptly close to its end. Unlike *C. cambrica* (Chambi-Trowell *et al.* 2019) and *C. bairdi* (Sues *et al.* 1994, fig. 1B), there is no posterior curvature of the maxillary dorsal process forming the antero-orbital margin; this shape is more akin to the maxilla of *Diphydontosaurus* (Whiteside 1986, fig. 4A). Unlike *Diphydontosaurus*, however, the suborbital process remains near uniform for much of its length rather than tapering. Posteriorly, the maxilla forms a ventrally positioned medial shelf that contacts the jugal and ectopterygoids. Dorsomedially, the maxilla is somewhat concave where it would have contacted the nasal and prefrontal.

Nasal. Only the left nasal (Fig. 11D–F) is preserved, and the anterior portion is damaged. The nasals are large and elongated compared to those in the short robust snouts of *Clevosaurus* and more like those of *Diphydontosaurus*, *Gephyrosaurus* or *Planocephalosaurus* (Evans 1980; Fraser 1982; Whiteside 1986). The nasals are less convex than those of *C. brasiliensis*, reflecting a long rostrum positioned at a shallower angle.

Prefrontal. The prefrontal (Fig. 11D–F) appears relatively typical for rhynchocephalians, with a roughly lunate shape and a broad lateral contact with the maxilla, and medially with the nasal. Ventrally it contacts the palatine, but probably not the jugal unlike in *C. brasiliensis*. It has sustained some damage on its dorsolateral surface.

Postfrontal. The anterior process of the postfrontal (Fig. 11G, H) is long and columnar, as in *Planocephalosaurus* and *Diphydontosaurus* (Fraser 1982; Whiteside 1986), while the posterior process appears to be very short to non-existent, but may simply be damaged, and the ventral process is bifurcated, with a deep groove into which the postorbital would have articulated. This 'four-cornered' postfrontal with a deep
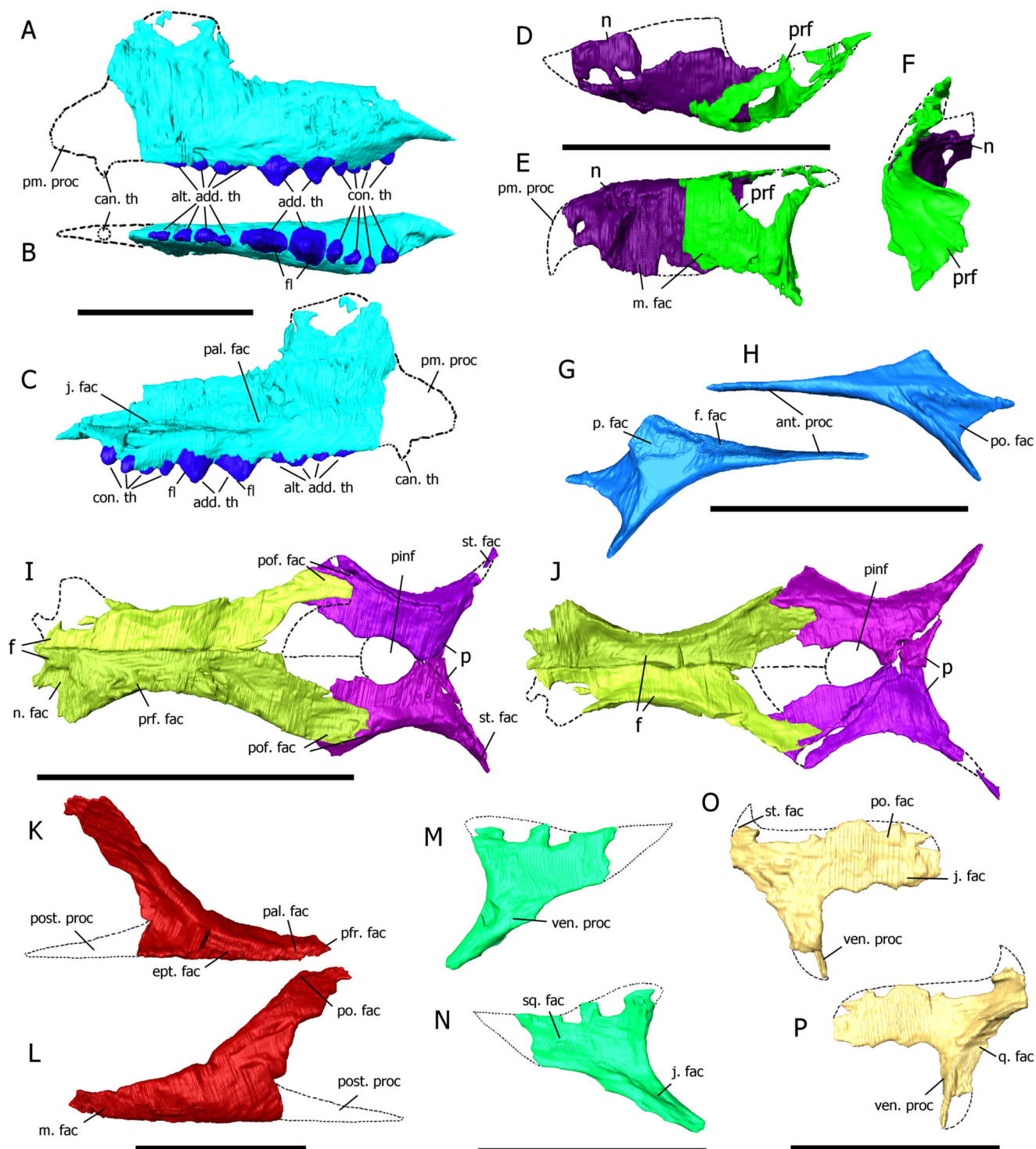
Figure 11. Digital segmentation of selected cranial material of the holotype of *Microsphenodon bonapartei* gen. et sp. nov. (UFRGS-PV-0972-T). **A–C,** left maxilla in: **A,** lateral; **B,** ventral; and **C,** medial views. **D–F,** left nasal and prefrontal in: **D,** dorsal; **E,** lateral; and **F,** posterior views. **G, H,** left postfrontal in: **G,** medial; and **H,** lateral views. **I, J,** articulated frontals and parietals in: **I,** dorsal; and **J,** ventral views. **K, L,** left jugal in: **K,** lateral; and **L,** medial views. **M, N,** left postorbital in: **M,** medial; and **N,** lateral views. **O, P,** right squamosal in: **O,** lateral; and **P,** medial views. **Abbreviations: add**, additional; **alt**, alternating; **ant**, anterior; **can**, caniniform; **con**, conical; **ept**, epipterygoid; **f**, frontal; **fac**, facet; **fl**, flange; **j**, jugal; **m**, maxilla; **n**, nasal; **p**, parietal; **pal**, palatine; **pfr**, prefrontal; **pinf**, pineal foramen; **pm**, premaxilla; **po**, postorbital; **pof**, postfrontal; **post**, posterior; **prf**, prefrontal; **proc**, process; **q**, quadrate; **sq**, squamosal; **st**, supratemporal; **th**, tooth; **ven**, ventral. Scale bars for A–H, K–P equal 5 mm; I, J equal 10 mm.
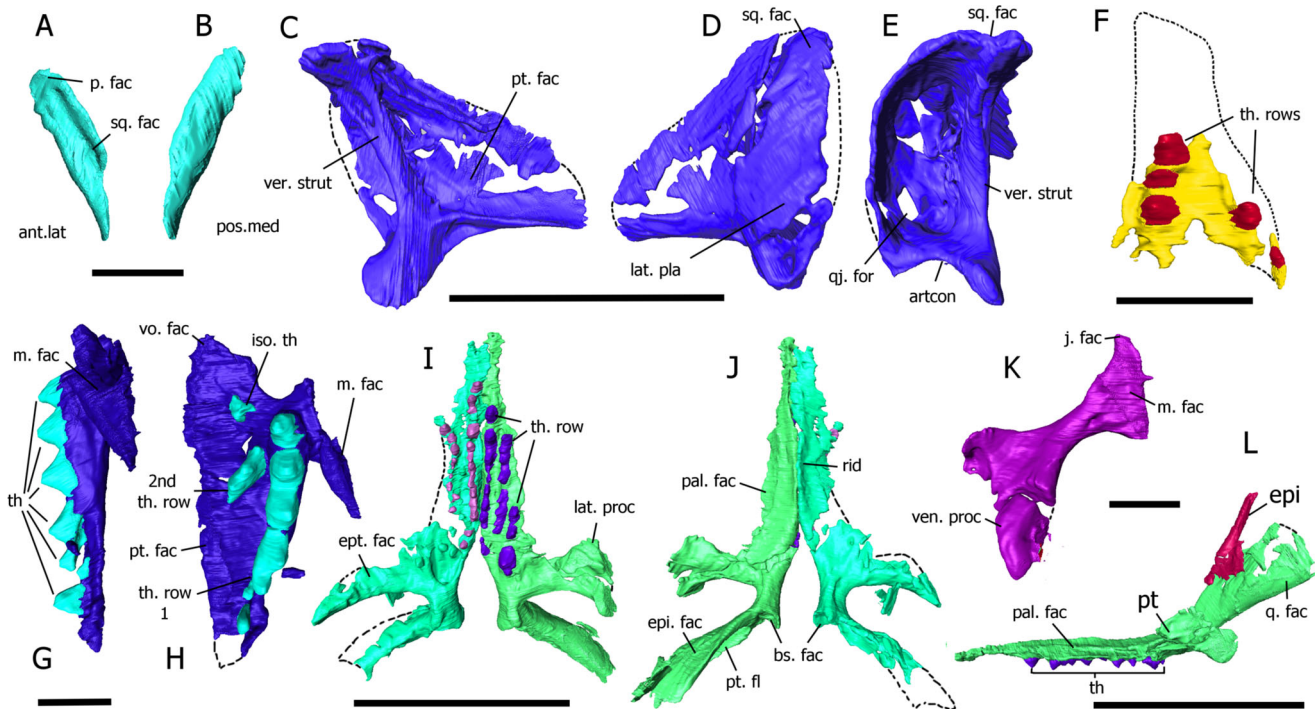
Figure 12. Digital segmentation of selected cranial material of the holotype of *Microsphenodon bonapartei* gen. et sp. nov. (UFRGS-PV-0972-T). **A, B,** left supratemporal in: **A,** dorsal; and **B,** ventral views. **C–E,** left quadrate in: **C,** medial; **D,** lateral; **E,** posterior views. **F,** left vomer in ventral view. **G, H,** left palatine in: **G,** lateral; and **H,** ventral views. **I, J,** pterygoids in: **I,** ventral; and **J,** dorsal views. **K,** left ectopterygoid in ventral view. **L,** left pterygoid and epipterygoid in lateral view. **Abbreviations: ant,** anterior; **artcon,** articular condyle; **bs,** basisphenoid; **epi,** epipterygoid; **ept,** ectopterygoid; **fac,** facet; **fl,** flange; **for,** foramen; **iso,** isolated; **j,** jugal; **lat,** lateral; **m,** maxilla; **med,** medial; **p,** parietal; **pal,** palatine; **proc,** process; **pt,** pterygoid; **q,** quadrate; **qj,** quadratojugal; **rid,** ridge; **sq,** squamosal; **th,** tooth; **ven,** ventral; **ver,** vertical; **vo,** vomer. Scale bars for A, B, F–H, K equals 1 mm; C, D, I, J, L equals 5 mm.

groove is very similar in shape to that of *C. minor* (Fraser 1988, fig. 39).

Frontal. The frontals (Fig. 11I, J) are not fused, unlike those of basal rhynchocephalians (Evans 1980; Fraser 1982; Whiteside 1986). Rather, they are paired, forming an hourglass shape, with two long posterior flattened processes that overlap the parietals dorsally. Anterodorsally there are facets for the prefrontals and nasals.

Parietal. The parietals (Fig. 11I, J) form a broad and relatively short flat parietal table, and they are paired, unlike the fused elements of some basal rhynchocephalians (Evans 1980; Fraser 1982; Whiteside 1986); the fusion is late in ontogeny in *Diphydontosaurus* according to Whiteside (1986). The posterior process on each parietal is short and tapers rapidly, with a distinctive slot on its dorsal surface for the supratemporal where it overlay both the parietal and quadrate.

Jugal. The jugal (Fig. 11K, L) formed a broad contact with the ectopterygoid medioventrally and with the maxilla laterally. It contacted the palatine anteriorly. The

bone formed a broad contact with the postorbital along the lateral surface of its dorsal process, which also overlay the squamosal ventrally. The jugal did not interdigitate with the postorbital unlike *C. brasiliensis*. The posterior process is missing in all specimens.

Postorbital. The postorbital (Fig. 11M, N) is a triradiate bone that laterally overlapped the squamosal and jugal. The ventral process would have partially wrapped around the jugal along its lateral surface, a condition shared with European *Clevosaurus* (Fraser 1988; Chambi-Trowell *et al*. 2019) but differing from the interdigitating condition seen in the jugal in *C. brasiliensis*.

Squamosal. The squamosal (Fig. 11O, P) is generally typical of *Clevosaurus* (see Fraser 1988). There is some damage to the ventral process, but most of the bone is preserved. The ventral process is not curved or as broad as in *C. brasiliensis*. The lateral surfaces of both squamosals are damaged, so it is unclear whether there was a similar lateroventral depression as in *C. brasiliensis*.

Supratemporal. The supratemporal (Fig. 12A, B) is a small, convex, plate-like bone that connects the
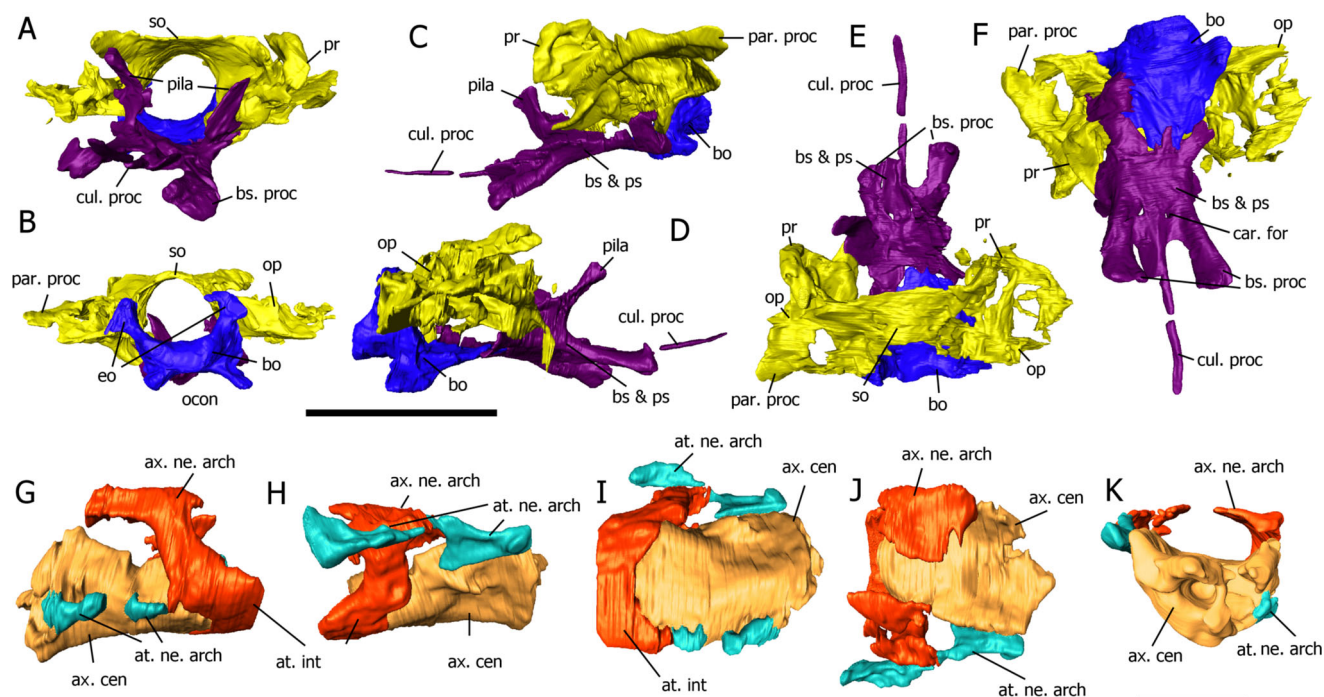
Figure 13. The braincase and cervical vertebra of *Microsphenodon bonapartei* gen. et sp. nov. (UFRGS-PV-0972-T). **A–F,** near-complete braincase in: **A,** anterior; **B,** posterior; **C,** left lateral; **D,** right lateral; **E,** dorsal; and **F,** ventral views. **G–K,** fragments of the axis and atlas in: **G,** right lateral; **H,** left lateral; **I,** ventral; **J,** dorsal; and **K,** posterior views. **Abbreviations: at,** atlas; **ax,** axis; **bo,** basioccipital; **bs,** basisphenoid; **car. for,** carotid foramen; **cen,** centrum; **cul. proc,** cultriform process; **eo,** exoccipital; **int,** intercentrum; **ne. arch,** neural arch; **ocon,** occipital condyle; **op,** opisthotic; **par,** paroccipital; **pila,** pila antotica; **pr,** prootic; **proc,** process; **ps,** parasphenoid; **so,** supraoccipital. Scale bars for A–F equal 5 mm; G–K equal 1 mm.

squamosal to the parietal, with a ridge on its ventral side that articulates with both. It is roughly rectangular in profile, and midway along its long axes there is a parallel indentation, possibly indicating a site for attachment of the M. depressor mandibulae. Supratemporals have not been confirmed previously in any rhynchocephalians except clevosaurs (Jones 2006; Chambi-Trowell *et al.* 2020). The supratemporal may be damaged posteriorly, and it is unclear whether it articulated with the paroccipital process as in *C. brasiliensis*.

Quadrate. The overall shape of the quadrate (Fig. 12C–E) shares some similarity with *C. brasiliensis*, but it is far less robust, with a pronounced curved ventral condyle that is angled at roughly 45° to the vertical strut in medial view, resulting in a more posteriorly positioned dorsal condyle. The medially positioned shelf along the ventral edge of the quadrate flange is pronounced but flat and not curved dorsally as in *C. brasiliensis*. The bone is very porous around the condyles. A quadratojugal cannot be distinguished from the quadrate, and the quadratojugal foramen is small compared to that of *Sphenodon punctatus* and positioned ventrolaterally.

Vomer. No complete vomer is known. Only a fragment of the left vomer, articulated with the palatine, is preserved in the holotype (Fig. 12F). It bears two rows of teeth, one central row with three teeth preserved and one lateral with two teeth preserved. Other disarticulated teeth are found separately in the matrix. Numerous teeth on the vomer are a character typical of basal rhynchocephalians such as *Gephyrosaurus*, *Planocephalosaurus* and *Diphydontosaurus* (Evans 1980; Fraser 1982; Whiteside 1986), but two rows are also observed in *C. brasiliensis*.

Palatine. The palatine (Figs 4C, 6E–G, 12G, H) is distinct, bearing a slightly curved lateral row of six teeth (Fig. 12G), a single medially placed tooth, and a fused row of two teeth (Fig. 12H) that are angled at roughly 45° to the lateral row (Figs 4C, 6E–G). This condition of a short, angled secondary row of teeth is seen also in *Rebbanasaurus* (Evans *et al.* 2001) though that taxon has three rather than two teeth. The isolated medially positioned tooth is characteristic of *Clevosaurus* (Fraser 1988; Klein *et al.* 2015; Chambi-Trowell *et al.* 2019), but not *Clevosaurus brasiliensis*. The six teeth in the lateral row are significantly fewer than observed in *Gephyrosaurus*, *Planocephalosaurus* and *Diphydontosaurus* (Evans 1980; Fraser 1982; Whiteside 1986) and more similar to *C. cambrica*, *C. hudsoni* and

C. sectumsemper (Fraser 1988; Klein *et al*. 2015; Chambi-Trowell *et al*. 2019). There is a lateral groove on the palatine between the lateral tooth row and the maxillary process, as previously noted (Romo de Vivar Martínez & Soares 2015; Romo-de-Vivar-Martínez *et al*. 2019). The maxillary process would likely have had a broad contact with the maxilla in life but the anterior part of the maxillary process has broken off. Posteriorly, the maxillary process contacts the ectopterygoid and jugal. The palatine articulates posteriorly on its dorsal surface with the ectopterygoid, and with the pterygoid along its medial ventral surface, excluding the pterygoid from the suborbital fenestra. This differs from the condition in non-eusphenodontians (Evans 1980; Fraser 1982; Whiteside 1986); however, the pterygoid has only the slightest contact with the suborbital fenestra in the reconstruction of *Diphydontosaurus* by Whiteside (1986, fig. 3b).

Pterygoid. The pterygoid (Fig. 12I, J, L) bears three rows of teeth, the third row being very short and consisting of just three teeth, as in *C. brasiliensis*, *Brachyrhinodon* and *Planocephalosaurus* (Fraser 1982). There is an interdigitating facet between the pterygoids anteriorly, and dorsally there is a raised ridge of bone on either side of this facet, but this is not as pronounced as in *C. brasiliensis*. The ramus between the start of the pterygoid flange and the lateral process is shorter than that of *Sphenodon* (Evans 2008) but is relatively longer and narrower than in *C. brasiliensis*. The pterygoid lateral processes widen laterally and articulate ventrally with the ectopterygoids. The basipterygoid facets are cup-like.

Ectopterygoid. The ectopterygoid (Fig. 12K) closely resembles that of *C. brasiliensis* but has a relatively longer, more gracile maxillary process and a shorter ventral process.

Epipterygoid. The epipterygoid (Fig. 12L) is rod-like dorsally and wider and more flattened ventrally where it articulates with the pterygoid flange. It is nearly identical to that of *C. brasiliensis* and other clevosaurs where this has been described, as well as *Gephyrosaurus* and *Diphydontosaurus* (Evans 1980; Whiteside 1986; Sues *et al*. 1994; Chambi-Trowell *et al*. 2019, fig. 8C).

Parabasisphenoid. The parasphenoid and basisphenoid are fused (Fig. 13A–F), forming the floor of the braincase, which is much narrower than in *C. brasiliensis*. Anteriorly, there are two elongate basipterygoid processes that widen anteriorly and articulate with the pterygoids. The cultriform process is elongate and reaches at least as far as the end of the interpterygoid vacuity.

There are two carotid foramina, one on each side of the base of the cultriform process (Fig. 13F).

Basioccipital-exoccipitals. The basioccipitals and exoccipitals are fused (Fig. 13A–F), as in *Gephyrosaurus*, *Planocephalosaurus* and *Diphydontosaurus* (Evans 1980; Fraser 1982; Whiteside 1986) and differing from the condition in *C. brasiliensis* and other clevosaurs. The exoccipitals would have formed more than 50% of the foramen magnum. The basal tubera are short and project posteroventrally. The occipital condyle is lunate in shape, with a slightly raised medial ridge positioned just anteriorly of the condyle, as in *Diphydontosaurus* (Whiteside 1986, fig. 26a). The basioccipital articulates with the dorsal surface of the parabasisphenoid.

Opisthotics, prootics and supraoccipital. These bones (Fig. 13A–F) cannot be distinguished in the scans, and it is possible all three were fused, forming the roof of the braincase, as observed in *C. hudsoni* (Fraser 1988, p. 140; O'Brien *et al*. 2018; Chambi-Trowell *et al*. 2019) and *C. brasiliensis*. The roof of the braincase appears to have a much lower bone density than the rest of the skull and as a result is hard to distinguish from the matrix, a feature in common with *C. cambrica* and *C. hudsoni* (O'Brien *et al*. 2018; Chambi-Trowell *et al*. 2019) and *C. brasiliensis*. The supraoccipital forms part of the dorsal margin of the foramen magnum, and its dorsal surface is broad and relatively flat, with no dorsal crest present. The pila antotica is similar in shape to that of *Clevosaurus*, lateromedially flattened and curving dorsally, widening to a squared-off head.

Dentary. The dentaries (Fig. 8F–H, L) are relatively long and narrow, with a high coronoid process and they have the pronounced edentulous region between the ultimate tooth and coronoid process often seen in clevosaurs and in *Diphydontosaurus* and *Planocephalosaurus* (Fraser 1982; Whiteside 1986; Fraser 1988; Fraser & Benton 1989; Sues *et al*. 1994; Chambi-Trowell *et al*. 2019). As in most rhynchocephalians, there is a raised lip of secondary bone on the lateral surface of the dentary. The symphysis is long and slants anterodorsally at a low angle, and seemingly lacks the medially positioned post-symphyseal lamina seen in *Lanceirosphenodon* (Romo de Vivar *et al*. 2020a, fig. 5). The dentary has pronounced diagonal wear facets from the maxillary teeth, as often seen in *Clevosaurus* (Fraser 1988; Klein *et al*. 2015; Chambi-Trowell *et al*. 2019), as well as *Diphydontosaurus*, but not present in *C. brasiliensis*. The anterior-most region of the dentary appears to be edentulous (but as the scanned holotype has damage in this region of the jaw, we cannot verify this). There appears to be a single caniniform, followed
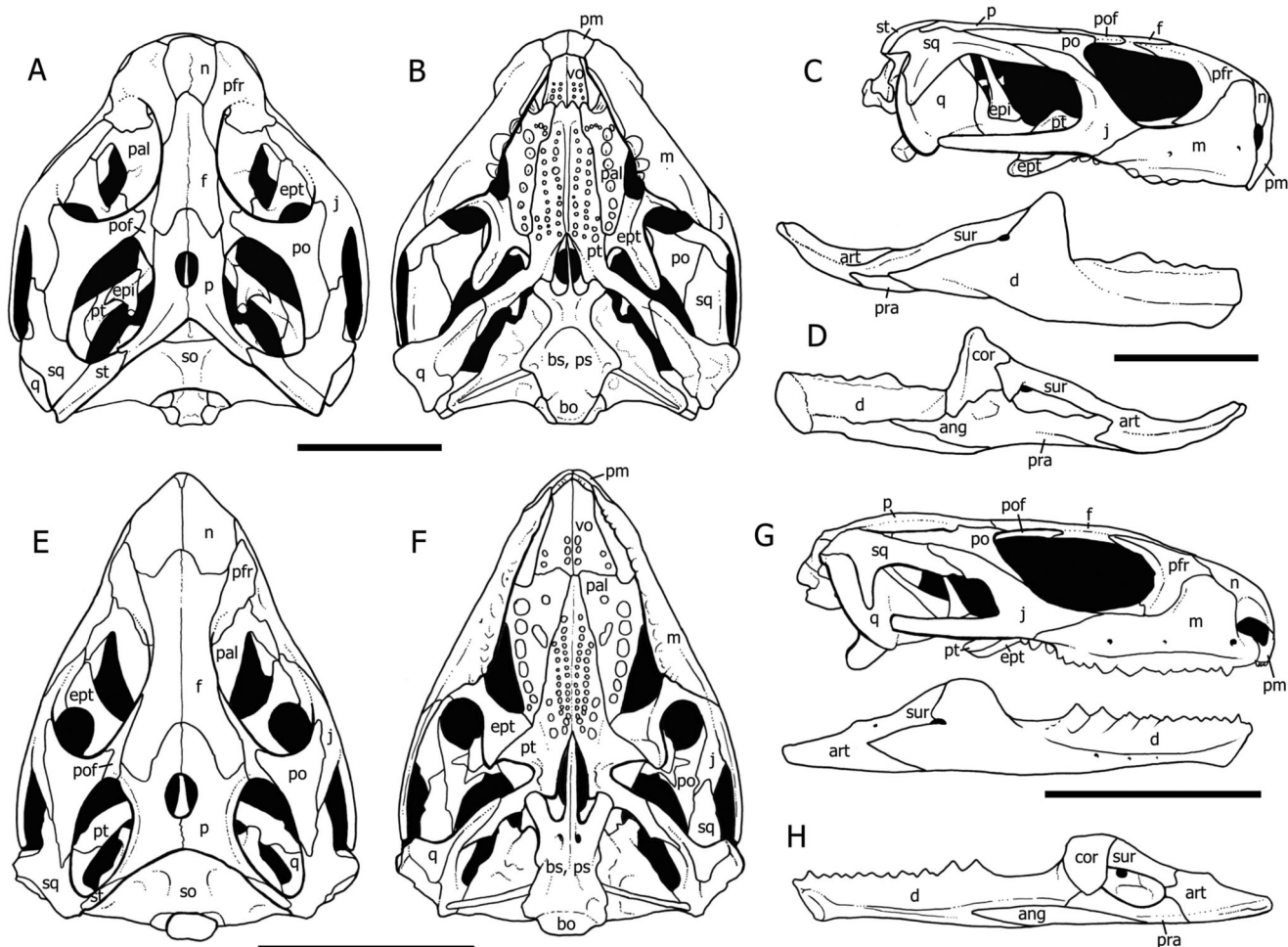
Figure 14. Reconstructions of the skulls of *Clevosaurus brasiliensis* (**A–D**) and *Microsphenodon bonapartei* gen. et sp. nov. (**E–H**). **A, B,** cranium of *C. brasiliensis* in: **A,** dorsal; **B,** ventral views. **C,** right lateral view of the cranium and mandible of *C. brasiliensis*. **D,** a medial view of the right mandible of *C. brasiliensis*. **E, F,** cranium of *M. bonapartei* in: **E,** dorsal, **F,** ventral views. **G,** a right lateral view of the cranium and mandible of *M. bonapartei*. **H,** a medial view of the right mandible of *M. bonapartei*. **Abbreviations: ang**, angular; **art**, articular; **bo**, basioccipital; **bs**, basisphenoid; **cor**, coronoid; **d**, dentary; **epi**, epipterygoid; **ept**, ectopterygoid; **f**, frontal; **j**, jugal; **m**, maxilla; **n**, nasal; **p**, parietal; **pal**, palatine; **pm**, premaxilla; **po**, postorbital; **pof**, postfrontal; **pfr**, prefrontal; **pra**, prearticular; **ps**, parasphenoid; **pt**, pterygoid; **q**, quadrate; **so**, supraoccipital; **sq**, squamosal; **st**, supratemporal; **sur**, surangular; **vo**, vomer. Scale bars equal 10 mm.

by 4–5 hatchling teeth, then 4–6 teeth that alternate in size, increasing in size posteriorly (Fig. 8F, G; UFRGS-PV-0613-T, Romo de Vivar Martínez & Soares 2015, fig. 3C, 4F), and finally there are two large flanged mesiodistally elongated teeth with roughly triangular lateral profile. There are no escape structures, and rather like *Lanceirosphenodon* (Romo de Vivar *et al*. 2020a), the teeth have a convex lingual surface with the cusp deflected lingually. Like *C. convallis*, the hatchling teeth remain visible in adult specimens.

Coronoid. The coronoid (Fig. 8F–H) is a small, thin bone; it is unclear whether it projected above the dentary.

Articular complex (prearticular, surangular and articular) and angular. The articular complex (Fig. 8D–F) appears to be fused, as the facets between the bones are indistinguishable from one another. The angular is flattened and reaches as far anteriorly as the posterior-most tooth of the dentary. The mandibular foramen is formed between the surangular and dentary and is large, unlike that of *C. brasiliensis*. The dorsal surface of the surangular is also very wide and robust compared to other rhynchocephalians, and the articular is robust, with a remarkably long retroarticular process that forms a spoon-like structure that tapers posteriorly and is deepest laterally, as in *C. brasiliensis*. The articular condyle is full of porous bone. The fusion of the
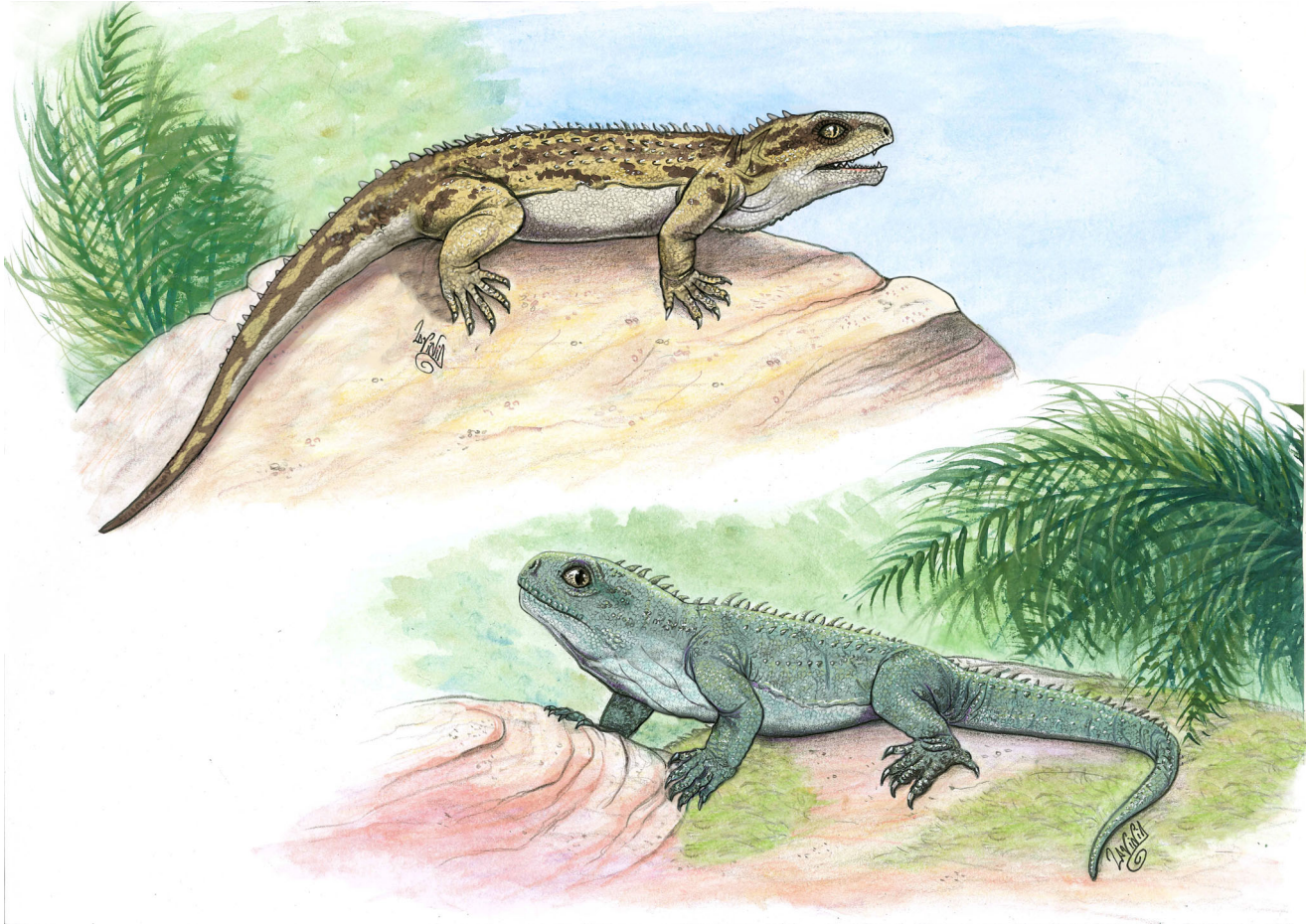
Figure 15. Life reconstruction of *Microsphenodon bonapartei* gen. et sp. nov. (top left) and *Clevosaurus brasiliensis* (bottom right). Work by Lavinia Gandolfi.

prearticular, articular and surangular in *Microsphenodon* is an important difference from *Clevosaurus brasiliensis* but a feature shared with early diverging rhynchocephalians such as *Gephyrosaurus*, *Diphydontosaurus* and *Planocephalosaurus.*

Additional and postcranial material. Among the holotype material, long rod-like elements are observed beneath the skull (Fig. 10D), inferred to be remnants of the hyoid apparatus. Likewise, we also found very thin broken fragments of bone behind both orbits (Fig. 10A, C), which we suggest are fragments of the sclerotic ossicles. The axis and atlas are present (Fig. 13G–K), but the former has sustained considerable damage dorsally so that much of the neural arch is missing and only the centrum of the axis remains intact. The centrum of the atlas is fused to that of the axis, forming the odontoid process which articulates dorsally to the atlas intercentrum. The axis intercentrum is possibly preserved, but the suture lines

between it and the atlas intercentrum cannot be distinguished in the scans and only the atlas intercentrum is prominent. The atlas/axis complex has a similar configuration to that in basal rhynchocephalians such as *Gephyrosaurus* (Evans 1981, fig. 2) and eusphenodontians like *Sphenodon*.

Reconstructions

The anatomy of the two Brazilian taxa has been presented in some detail based on µCT scans, and we offer standardized skull drawings of both (Fig. 14). The detail is based entirely on the fossils, and, because of their completeness, we had to make very few assumptions or restorations of missing parts. In the case of *Clevosaurus brasiliensis* (Fig. 14A–D), it lacks a complete vomer, as well as the stapes. In the case of *Microsphenodon bonapartei* (Fig. 14E–H), the posterior process of the jugal is broken off, only a small portion of the left vomer is preserved and it is missing the premaxillae and stapes. The

whole-body life drawings (Fig. 15) represent the head shapes according to the fossil data, but the body shapes are speculative.

Phylogenetic results

The maximum parsimony analysis (Fig. 16A) retained four trees with lengths of 669 steps (consistency index, CI = 0.297; retention index, RI = 0.634), the results of which were summarized in a strict consensus tree. The Bayesian analysis output was summarized as an MRC tree, as the strict tree collapsed to form a large polytomy. The Bayesian MRC tree (Fig. 16B) generally resembles the parsimony analysis but has lower resolution within Eusphenodontia. Both analyses show good resolution of the outgroup, basal taxa, Pleurosauridae, Eilenodontinae, Opisthodontia, Eusphenodontia, Clevosauridae and Acrosphenodontia (new clade). The maximum parsimony tree also shows good resolution of Neosphenodontia, Sphenodontidae, Sphenodontinae and Sapheosauridae. Support values are fairly low for many of the nodes but are similar or higher than in previous analyses where these values were stated (e.g. Apesteguía et al. 2012, 2014; Bever & Norell 2017; Herrera-Flores et al. 2018; Romo de Vivar et al. 2020a). Most nodes have a Bremer value of at least 1, but Pleurosauridae and Clevosauridae are both supported by a Bremer value of 4, the 'Solnhofen clade' is supported by a Bremer value of 2, and several of the early diverging taxa are supported by values higher than this (Fig. 16A).

In our trees, clevosaurs form a clade that excludes *Polysphenodon*, in agreement with previous studies (Herrera-Flores et al. 2018; Hsiou et al. 2019; Romo de Vivar et al. 2020a). Clevosaurs are recovered as the earliest diverging eusphenodontian group (see also Hsiou et al. 2015, 2019; Herrera-Flores et al. 2018; Romo de Vivar et al. 2020a; Simões et al. 2020). Among the clevosaurs, we find support for our previous proposal (Chambi-Trowell et al. 2019) that there are two morphotypes within *C. hudsoni*, which could indicate two separate species. *Clevosaurus brasiliensis*, as in previous analyses (Hsiou et al. 2015; Herrera-Flores et al. 2018), nests within *Clevosaurus*, but in our analyses we find it is closely related to *Brachyrhinodon* and *C. bairdii*, the three taking the earliest diverging position within Clevosauridae and forming a small subclade of their own. We found *C. convallis* to be the sister taxon to *Sigmala sigmala*, the two diverging prior to *Brachyrhinodon taylori*.

We recover *Microsphenodon bonapartei* as the earliest diverging member of Eusphenodontia after *Polysphenodon*.

Within Neosphenodontia, we find some results that differ from those in previous analyses. Unlike previous analyses (e.g. Bever & Norell 2017), Opisthodontia, which was defined as "all sphenodonts that are more closely related to *Priosphenodon* than *Sphenodon*" (Apesteguía & Novas 2003, p. 611), includes the pleurosaurs. We found the genus *Opisthias* to be outside Opisthodontia and closer phylogenetically to *Sphenodon* than to *Eilenodontinae*. Despite the movement of these subclades, their composition remains very similar to previous findings, and we retain the clade Opisthodontia with its original definition, even though here it excludes *Opisthias*.

Earlier, we also proposed the new formal name Acrosphenodontia (see clade definitions).

Like Simões et al. (2020), we found that Pleurosauridae was more closely related to other Solnhofen taxa than to Sphenodontidae. Our 'Solnhofen subclade' does not include all taxa from these deposits, but as in Simões et al. (2020), it contains *Kallimodon*, *Sapheosaurus* and *Homoeosaurus*. As in previous analyses (Hsiou et al. 2015, 2019; Herrera-Flores et al. 2018; Romo de Vivar et al. 2020a), we recover *Kallimodon* and *Sapheosaurus* as sister taxa, forming the subclade Sapheosauridae.

Our phylogenetic analysis suggests some further changes in taxon affinities compared to earlier studies: both *Ankylosphenodon* and *Oenosaurus* move out of Sphenodontidae (Herrera-Flores et al. 2018; Hsiou et al. 2019; Romo de Vivar et al. 2020a), and join the branch leading to Eilenodontinae, which differs from Simões et al. (2020), who consider the latter to be a sapheosaurid.

Uniquely, our maximum parsimony analysis also recovers a small clade of seven taxa that diverges at the base of Neosphenodontia; however, we regard this clade with some scepticism because all these taxa are represented by potentially (but not definitively) immature specimens. Though we made efforts to avoid coding characters that might be affected by ontogeny (for example, excluding characters such as skull length and limb length ratios), ontogeny might have an influence on the position of these taxa. In *Sphenodon*, allometric changes through ontogeny mean that juveniles possess a relatively longer antorbital region, larger orbits, and smaller adductor chambers, as in early diverging non-eusphenodontians such as *Gephyrosaurus*, *Diphydontosaurus*, *Planocephalosaurus* and *Microsphenodon* (Jones & Lappin 2009). *Rebbanasaurus*, *Leptosaurus* and *Pamizinsaurus* all possess an enlarged lateral premaxillary tooth, which we otherwise find to be a unique character of Sphenodontinae. But as this clade is positioned basally to Sphenodontinae, it might be a plesiomorphic trait for Neosphenodontia.
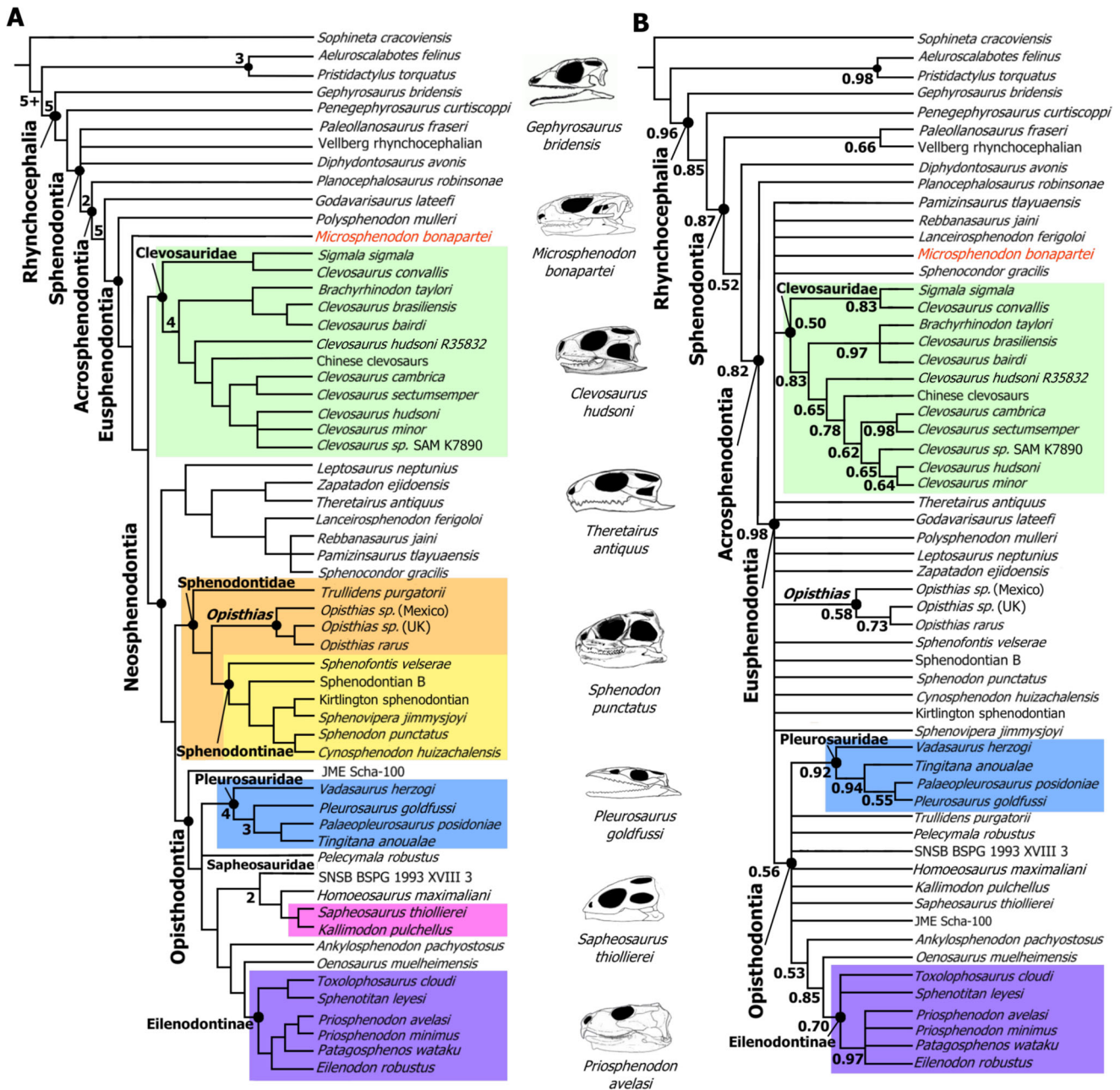
Figure 16. Phylogeny of Rhynchocephalia, recovered from: **A,** strict consensus tree from the maximum parsimony analysis with Bremer values above 1 labelled beside the nodes; and **B,** 50% majority rule consensus tree from the Bayesian-inference analysis with clade credibility values (decimal proportions) labelled beside nodes.

Discussion

Clevosaurus brasiliensis

Our anatomical observations and phylogenetic analysis (Fig. 16) confirm that *Clevosaurus brasiliensis* is an early diverging clevosaur, sharing several characteristics with *Brachyrhinodon taylori*, and together with *C. bairdii* forms a small subclade at the base of Clevosauridae. Unlike later clevosaurs, both

C. brasiliensis and *B. taylori* bear three rows of teeth on their pterygoids (SAVC-T, pers. obs.), the lateral-most of which is reduced to just two to three teeth. In addition, both taxa possess robust jaws, short snouts, broad skulls, a remarkably elongated retroarticular process, two to three large additional teeth on the maxilla, and a high coronoid process. Unfortunately, the nature of the implantation, tooth form, and number – features that mark *C. brasiliensis* as distinct from other *Clevosaurus*

– cannot be verified in *B. taylori* as these characteristics are not preserved.

The teeth of *C. brasiliensis* differ from those of later clevosaurs in morphology and implantation, appearing to be acrodont but nested deep within the jaw bones so that only a small portion of the tooth is visible. Rather than forming a jagged, narrow, semi-continuous blade, posteriorly the teeth of *C. brasiliensis* are closely packed and fused together, and both the cusps and dentary are worn at an angle as the animal ages. This means that the anterior hatchling teeth form a continuous narrow cropping beak-like structure. Most *Clevosaurus* species show additional dentary teeth with a mesiodistally elongated saddle shape and the cusp asymmetrically placed posteriorly on the tooth displaying large anterolateral flanges (Chambi-Trowell *et al.* 2020). However, the additional teeth of *C. brasiliensis* are mostly conical, with only the ultimate tooth – which can be up to two to three times bigger than any of the other teeth – elongated mesiodistally, and with its cusp placed anteriorly rather than posteriorly (two features unique to *C. brasiliensis* amongst clevosaurs, but also shared with *Planocephalosaurus*). In contrast to other clevosaurs, the teeth on the dentary of *C. brasiliensis* do not appear to bear flanges at all. But despite these differences, *C. brasiliensis* is otherwise very similar to later clevosaurs, with a short robust snout, broad skull, supratemporal bone, premaxillary beak and an elongated retroarticular process.

Some of the skull traits of *C. brasiliensis* suggest that it must have been capable of a strong bite, such as its robust and short snout that seems to be further reinforced by its brace-like premaxillae and the slot-like facet on the prefrontal so that the maxilla is supported both medially and laterally. A similar slot-like facet is observed between the postorbital and jugal, with the bone interdigitating along their meeting edge rather than the simpler overlapping facets seen in later clevosaurs.

Microsphenodon bonapartei

Originally considered to be the juvenile form of *Clevosaurus brasiliensis* (Bonaparte & Sues 2006; Romo de Vivar Martínez & Soares 2015), we note the following morphological differences that indicate it represents a different genus and species: fusion of articular, surangular and prearticular; fusion of exoccipitals and basioccipital; deep diagonal wear facets on dentary; lack of an enlarged posterior-most tooth on the dentary; two rows of teeth on the palatine (albeit one is rudimentary); elongated antorbital region of the skull; broad parietal table; four-cornered postfrontal; typical acrodonty (teeth sit on the jaw crest and do not extend deeply into the jaw bones); elongated premaxillary process on maxilla; short posterior process on the parietal; relatively gracile jaw; non-interdigitating facets between jugal-postorbital and maxilla-prefrontal; and presence of (small) caniniforms. All four specimens of *M. bonapartei* suggest an animal with a skull around 20 mm long, which is only slightly smaller than *C. brasiliensis* (with specimens averaging around 25 mm).

Our phylogenetic analysis (Fig. 16) recovered *Microsphenodon* as the earliest diverging eusphenodontian after *Polysphenodon*. Plesiomorphic features include its relatively elongated snout, fusion of the exoccipitals to the basioccipital, broad flat parietal table, low gracile dentary, and its multiple rows of palatal teeth, while apomorphies include its fully acrodont dentition, a high coronoid process, differentiated dentition, and a large parietal opening. The last character-state could be interpreted as evidence the specimen is juvenile, perhaps based on the wider, flatter parietals in juvenile *Sphenodon* compared to adults, but some cranial sutures in *Microsphenodon* appear to be well fused, and the parietal opening size varies substantially among extinct rhynchocephalians, being small in *Gephyrosaurus* and outgroups, and large in clevosaurs and most eusphenodontians.

The palate of *Microsphenodon* is its key diagnostic feature, bearing multiple rows of teeth on the vomers, palatines and pterygoids. Although there are more tooth rows than in most eusphenodontians, the number of rows is still fewer than in earlier diverging forms such as *Gephyrosaurus*, *Diphydontosaurus* and *Planocephalosaurus*. The palatine of *Microsphenodon* is similar to that of *Rebbanasaurus* from the Early Jurassic of India (Evans *et al.* 2001), both of which bear two rows of palatine teeth, one reduced to just two to three teeth and positioned at roughly 45° to the main row of teeth. Medially, the palatine bears a single tooth that is otherwise an apomorphy (a single tooth or cluster of teeth placed medially on the palatine) known only within clevosaurs, suggesting this feature was plesiomorphic to *Clevosaurus*, though it is also arguably known in *Sphenotitan* from the Rhaetian of Argentina (Martínez *et al.* 2013). Whether this single tooth is present in *Rebbanasaurus* is unknown because this part of the palatine is missing.

The marginal teeth of *Microsphenodon* show some resemblances to those of derived rhynchocephalians. For example, the dentary is like that of *Sphenocondor* from the Middle Jurassic of Argentina (Apesteguía *et al.* 2012), with a high but elongated and blunt coronoid process, a gracile elongated dentary ramus and similar complex tooth differentiation. There are a few large, mesiodistally elongated additional teeth, and anterior to this many smaller teeth alternating in size, and successional teeth located most anteriorly, including a caniniform. *Microsphenodon* differs from *Sphenocondor* in showing no evidence of any other successional teeth

anterior to the caniniform (Fig. 3C). The only known specimen of *Sphenocondor* has been identified as a juvenile because some of its dentary teeth alternate in size, but it is roughly the same size as all known specimens of *Microsphenodon*, and adult specimens of *Diphydontosaurus* similarly display alternation in tooth size, suggesting that this type of dentition is not restricted to juveniles. Likewise, adult specimens of *Sphenodon* also have additional teeth that alternate in size (Maisano 2001). Further, *Microsphenodon*, like *Sphenocondor*, also has caniniform teeth, a tooth form not known in any other sphenodontians before the Jurassic, and not outside Neosphenodontia. However, the dentary of *Sphenocondor* also differs from *Microsphenodon* in seemingly possessing a large incisiform tooth and lacking the pronounced gap between the coronoid process and teeth (see below for further explanation).

It is important to compare *Microsphenodon* with *Lanceirosphenodon* (Romo de Vivar *et al.* 2020a), also from the *Riograndia* AZ (Candelária Sequence) of the Linha São Luiz outcrop in southern Brazil. *Lanceirosphenodon* resembles *Microsphenodon*, but there are several apomorphies that distinguish the two taxa. While the holotype and associated specimens of *Microsphenodon* are believed to represent adult individuals of a similar size, it is probable that *Lanceirosphenodon* is based on a juvenile holotype, with the distance between the symphysis to the coronoid process being $\sim$7.1 mm, making it approximately two-thirds the size of *Microsphenodon*. The pronounced gap between the ultimate tooth and the coronoid process of *Microsphenodon*, seen in other early sphenodontians including *Diphydontosaurus*, *Planocephalosaurus* and *Clevosaurus* spp. (Fraser 1982, pl. 70 (2); Whiteside 1986, fig. 4B; Fraser 1988, fig. 19), is absent in *Lanceirosphenodon*. This gap does not relate to ontogeny as it is present throughout life in *Clevosaurus hudsoni* (Fraser 1988, fig. 23). There also appear to be two series of alternating teeth on the dentary of *Lanceirosphenodon* (Romo de Vivar *et al.* 2020a, fig. 4B), one apparently representing the hatchling teeth and the other the larger additional teeth, but there is only one such series in *Microsphenodon*. *Lanceirosphenodon* also lacks pronounced diagonal wear facets on its dentary, but this could reflect its young age. Further, though both *Lanceirosphenodon* and *Microsphenodon* share the trait of two large additional teeth most posteriorly on the dentary following a row of additional teeth that alternate in size, their teeth differ in shape. The two largest posterior teeth of *Microsphenodon* are mesiodistally elongated with an equidistant triangular profile, while those of *Lanceirosphenodon* are more conical (Romo de Vivar *et al.* 2020a, fig. 4). If

Lanceirosphenodon is a juvenile, then it likely would have had more of these larger additional teeth as an adult. The maxilla of *Clevosaurus brasiliensis* possesses two large, additional teeth (Fig. 3D), so the possession of two large posterior-most teeth in the maxilla and dentary might have been a plesiomorphic trait for the rhynchocephalians of this Assemblage Zone.

Phylogenetic analysis and rhynchocephalian clade definitions

Our phylogenetic analysis (Fig. 16) confirms many broad features found in earlier studies, but also suggests some substantial rearrangements in the relationships between subclades within Neosphenodontia. The repeated discovery of key subclades within Rhynchocephalia, including Eusphenodontia, Neosphenodontia, Clevosauridae, Pleurosauridae, Opisthodontia, Eilenodontinae and Sphenodontidae, confirms some measure of stability. However, incomplete specimens and long temporal gaps pose challenges for improvement in confidence in the phylogenies.

To date there have been 10 proposed clades and subclades within Rhynchocephalia. Simões *et al.* (2020) reorganized clade nomenclature of rhynchocephalians, redefining several clades, but not all their definitions are compatible with our results. Below, we discuss this and their suggestion that Sphenodontia and Rhynchocephalia should be treated as synonymous. Differences in the phylogenetic topologies discovered by Simões *et al.* (2020) and in our analyses can be explained by differences in the character and taxon choice. When we ran our analysis with the same taxa as in Simões *et al.* (2020) but using our characters, we recovered a very similar topology to theirs (Supplemental Fig. 6) which is compatible with the findings below, but we did not recover *Derasmosaurus* as a pleurosaur. The strict maximum parsimony tree from this pruned matrix is (except for Pleurosauridae) compatible with the redefinitions they suggested. We therefore emphasise the importance of taxon selection for phylogenetic tree topology and suggest that future analyses consider all rhynchocephalians.

In the sequence of clade definitions below, we begin with the standard proposals by de Queiroz & Gauthier (2020) and Gauthier & de Queiroz (2020), as well as some earlier definitions, all cited, and differentiate node-based and stem-based definitions.

1. Lepidosauria Haeckel, 1866
   a. Definition: "The smallest crown clade containing *Lacerta agilis* Linnaeus, 1758 (*Squamata*) and *Sphenodon* (originally *Hatteria*) *punctatus* (Gray, 1842) (*Rhynchocephalia*)" (de Queiroz & Gauthier 2020, p. 1079). Node-based definition.

b. Remarks: de Queiroz & Gauthier (2020) give a very full account of the history and current nomenclature of this major diapsid clade.

2. Pan-Squamata Gauthier & de Queiroz, 2020
   a. Definition: "The total clade of the crown clade *Squamata*" (Gauthier & de Queiroz 2020, p. 1087). This is a stem-based definition, when expressed more fully, as "Squamata and all extinct species that are more closely related to that crown clade than they are to *Sphenodon punctatus*" (Gauthier & de Queiroz 2020, p. 1087).
   b. Remarks: Gauthier & de Queiroz (2020) give a very full account of the history and current nomenclature of crown clade Squamata, and the derivation of the name of the total clade Pan-Squamata.

3. Rhynchocephalia Günther, 1867
   a. Definition: "the most inclusive lepidosaurian clade including *Sphenodon* and *Gephyrosaurus*, but not *Iguana iguana* and *Gekko gecko*" (Simões *et al.* 2020, p. 12). Stem-based definition.
   b. Remarks: Simões *et al.* (2020) suggested that Sphenodontia and Rhynchocephalia should be synonyms as they found the position of *Gephyrosaurus* to be unstable in some of their analyses, but we find good support for *Gephyrosaurus* as a sister taxon to Sphenodontia in both our maximum parsimony and Bayesian analyses, and so retain the distinction between Rhynchocephalia and Sphenodontia. This stem-based clade matches Pan-Squamata, also stem-based, and together forming Lepidosauria, with a node-based definition.

4. Sphenodontia Williston, 1925
   a. Definition: The least inclusive clade including *Sphenodon*, *Diphydontosaurus* and the Vellberg jaw. It includes all known rhynchocephalians except *Gephyrosaurus* and *Penegephyrosaurus*. New, node-based clade definition.
   b. Remarks: All sphenodontians have some degree of acrodonty and lack a lacrimal.

5. Eusphenodontia Herrera-Flores *et al.*, 2018
   a. Definition: "The least inclusive clade containing *Polysphenodon muelleri*, *Clevosaurus hudsoni*, and *Sphenodon punctatus*" (Herrera-Flores *et al.* 2018, p. 740). Node-based definition.
   b. Remarks: All possess fully acrodont teeth, and in general have shorter antorbital and larger postorbital regions.

6. Neosphenodontia Herrera-Flores *et al.*, 2018
   a. Definition: "The most inclusive clade containing *Sphenodon punctatus* but not *Clevosaurus hudsoni*" (Herrera-Flores *et al.* 2018, p. 740). Stem-based definition.
   b. Remarks: The members of this clade generally have a narrower parietal table than interorbital width, sometimes possess sagittal crests and may at times completely lack a jugal posterior process.

7. Clevosauridae Bonaparte & Sues, 2006
   a. Definition: "All taxa more closely related to *Clevosaurus* than to *Sphenodon*" (Hsiou *et al.* 2015, p. 4). Stem-based definition.
   b. Remarks: Clevosaurs in general have a greatly reduced number of additional teeth compared to other clades and subclades, and often have distinctive saddle-shaped additional teeth on their dentaries. They all possess supratemporal bones, but these likely existed in early non-eusphenodontians, and are known in *Microsphenodon*. All clevosaurs possess a medially positioned isolated tooth, or cluster of teeth, on the palatine. Like earlier diverging genera, Clevosauridae (excluding *C. brasiliensis*) still possess a pronounced anterior alveolar foramen on their maxillae.

8. Pleurosauridae Lydekker, 1880
   a. Definition: The least inclusive clade containing *Vadasaurus herzogi*, *Palaeopleurosaurus posidoniae* and *Pleurosaurus goldfussi*. New, node-based definition.
   b. Remarks: Simões *et al.* (2020, p. 12) redefined Pleurosauridae as "The least inclusive clade containing *Palaeopleurosaurus posidoniae*, *Pleurosaurus goldfussi*, and *Derasmosaurus pietraroiae*", but our analysis suggests that *D. pietraroiae* is not a pleurosaur. All known pleurosaurs appear to have only one premaxillary tooth per premaxilla, which in earlier diverging forms projects prominently below the jaw. All but *Vadasaurus* have in excess of 25 presacral vertebrae.

9. Sapheosauridae Nopcsa, 1923
   a. Definition: The most inclusive clade that contains *Kallimodon* and *Sapheosaurus*. New, node-based definition.
   b. Remarks: Simões *et al.* (2020, p. 12) defined this clade as "the least inclusive clade containing *Sapheosaurus thiollerei*, *Piocormus laticeps*, and *Oenosaurus muehlheimensis*", but in our analysis *O. muehlheimensis* is more closely related to the eilenodontids than other

sapheosaurs, so their definition is therefore not supported here. The new definition is in line with our phylogenetic analysis and that of Herrera-Flores *et al*. (2018).

10. Opisthodontia Apesteguía & Novas, 2003
    a. Definition: "All the sphenodonts that are more closely related to *Priosphenodon* than *Sphenodon*" (Apesteguía & Novas 2003, p. 611). Stem-based definition.
    b. Remarks: We note that sphenodontians within this clade lack variation in their maxillary or dentary tooth morphology other than a decrease in size anteriorly. Generally, opisthodontians lack successional teeth and tend to lack a posterior process on the jugal. The maxilla is often excluded from the naris by the lateral process of the premaxilla, and all members possess a pronounced posterior process on the ischium where this has thus far been recorded.

11. Eilenodontinae Rasmussen & Callison, 1981
    a. Definition: The most inclusive clade containing *Eilenodon robustus*, *Sphenotitan* and/or *Toxolophosaurus*, but not *Sphenodon punctatus*. New, stem-based definition.
    b. Remarks: Rasmussen & Callison (1981) did not give a definition other than the clade should include both *Eilenodon robustus* and *Toxolophosaurus cloudi*. While the definition given by Simões *et al*. (2020, p. 12) is supported here ("The most inclusive clade containing *Eilenodon robustus*, but not *Sphenodon punctatus*"), we consider that *Sphenotitan* and *Toxolophosaurus* share enough similarities and are phylogenetically close enough that they should be included in this clade.

12. Sphenodontidae Cope, 1869
    a. Definition: All sphenodontians that are more closely related to *Sphenodon* than to *Priosphenodon*. New, stem-based definition.
    b. Remarks: This is a problematic clade because it has commonly been used without a clear definition and the composition has varied greatly. However, the new definition by Simões *et al*. (2020, p. 12), as "The most inclusive clade containing *Eilenodon robustus* and *Sphenodon punctatus*, but not *Kallimodon pulchellus* or *Saphaeosaurus thiollerei*" is not compatible with our analysis.

13. Sphenodontinae Nopcsa, 1928
    a. Definition: The most inclusive clade containing both *Sphenodon punctatus* and *Sphenofontis velseraei*. New, node-based definition.
    b. Remarks: Simões *et al*. (2020) redefined this as the most inclusive clade containing *Sphenodon punctatus*, but not *Eilenodon robustus*. This however is synonymous with our definition of Sphenodontidae, so we have added clarity. Members of this clade often have caniniforms, large/complete jugal posterior processes and an enlarged lateral tooth on their premaxilla (present in juvenile *Sphenodon* before premaxillary beak forms).

14. Acrosphenodontia new clade
    a. Definition: The most inclusive clade including *Planocephalosaurus robinsonae* and *Sphenodon punctatus*. New, node-based definition.
    b. Remarks: The teeth are fully acrodont, with no evidence of pleurodonty, except for some successional teeth in juvenile *Sphenodon*, and perhaps *Planocephalosaurus* and *Lanceirosphenodon* (see Fraser & Shelton 1988; Romo de Vivar *et al*. 2020a). It thereby excludes several earlier diverging sphenodontians. The name Acrosphenodontia means literally 'acrodont-toothed sphenodontians'.

Conclusions

We describe a new genus and species of eusphenodontian rhynchocephalian here, named *Microsphenodon bonapartei*, based on two remarkably well-preserved skulls and isolated cranial material, much of it previously referred to *Clevosaurus brasiliensis*. This new taxon shares a mosaic of features with the earliest rhynchocephalians and eusphenodontians, presenting the most complete articulated cranial remains of an early diverging sphenodontian from before the Rhaetian. We also establish a new clade name, Acrosphenodontia. In addition, we examine several remarkably well-preserved skulls of *Clevosaurus brasiliensis*, identifying new apomorphic features, including a unique modified form of acrodonty whereby the teeth are placed deep within the jaws in a continuous groove – future work will investigate the nature of tooth implantation in early Rhynchocephalia. The presence of three rhynchocephalians in the Norian of southern Brazil makes this locality uniquely informative in the understanding the early evolution of this group and of great significance in the of study small sized faunal components of the Late Triassic.

Acknowledgements

Supplemental material

Supplemental material for this article can be accessed here: https://doi.org/10.1080/14772019.2021.1976292.

ORCID

Sofia A. V. Chambi-Trowell http://orcid.org/0000-0003-1455-7347
Agustín G. Martinelli http://orcid.org/0000-0003-4489-0888
David I. Whiteside http://orcid.org/0000-0003-1619-747X
Paulo R. Romo de Vivar http://orcid.org/0000-0002-4959-6349
Marina Bento Soares http://orcid.org/0000-0002-8393-2406
Cesar L. Schultz http://orcid.org/0000-0001-7121-0409
Pamela G. Gill http://orcid.org/0000-0001-5957-3581
Michael J. Benton http://orcid.org/0000-0002-4323-1824
Emily J. Rayfield http://orcid.org/0000-0002-2618-750X

References

Andreis, R. R., **Bossi, G. E.** & **Montardo, D. K.** 1980. O Grupo Rosário do Sul (Triássico) no Rio Grande do Sul. Pp. 659–673 in *XXXI Congresso Brasileiro de Geologia. Volume 2*. SBG, Balneário de Camboriú.

Apesteguía, S. 2016. Rhynchocephalians: The least known South American lepidosaurs *Historia Evolutiva y Paleobiogeográfica de los Vertebrados de América del Sur. Contribuciones del MACN*, **6**, 7–19.

Apesteguía, S. & **Novas, F. E.** 2003. Large Cretaceous sphenodontian from Patagonia provides insight into lepidosaur evolution in Gondwana. *Nature*, **425**, 609–612.

Apesteguía, S., **Gómez, R. O.** & **Rougier, G. W.** 2012. A basal sphenodontian (Lepidosauria) from the Jurassic of Patagonia: new insights on the phylogeny and biogeography of Gondwanan rhynchocephalians. *Zoological Journal of the Linnean Society*, **166**, 342–360. doi:10.1111/j.1096-3642.2012.00837.x

Apesteguía, S. & **Carballido, J. L.** 2014. A new eilenodontine (Lepidosauria, Sphenodontidae) from the Lower Cretaceous of central Patagonia. *Journal of Vertebrate Paleontology*, **34**, 303–317.

Apesteguía, S., **Gómez, R. O.** & **Rougier, G. W.** 2014. The youngest South American rhynchocephalian, a survivor of the K–Pg extinction. *Proceedings of the Royal Society B*, **281**, 1–6.

Benton, M. J. 1985. Classification and phylogeny of the diapsid reptiles. *Zoological Journal of the Linnean Society*, **84**(2), 97–164.

Bever, G. S. & **Norell, M. A.** 2017. A new rhynchocephalian (Reptilia: Lepidosauria) from the Late Jurassic of Solnhofen (Germany) and the origin of the marine Pleurosauridae. *Royal Society Open Science*, **4**, 170570. doi:10.1098/rsos.170570

Bonaparte, J. F., **Ferigolo, J.** & **Ribeiro, A. M.** 1999. A new early Late Triassic saurischian dinosaur from Rio Grande do Sol State, Brazil. Pp. 89–109 in Y. Tomida, T. H. Rich & P. Vickers-Rich (eds) *Proceedings of the Second Gondwanan Dinosaur Symposium. National Science Museum Monographs*, **15**.

Bonaparte, J. F., **Ferigolo, J.** & **Ribeiro, A. M.** 2001. A primitive Late Triassic 'ictidosaur' from Rio Grande do Sul, Brazil. *Palaeontology*, **44**, 623–635. doi:10.1111/1475-4983.00194

Bonaparte, J. F., **Martinelli, A. G.**, **Schultz, C. L.** & **Rubert, R.** 2003. The sister group of mammals: small cynodonts from the Late Triassic of southern Brazil. *Revista Brasileira de Paleontologia*, **5**, 5–27. doi:10.4072/rbp.2005.1.03

Bonaparte, J. F., **Martinelli, A. G.** & **Schultz, C. L.** 2005. New information on *Brasilodon* and *Brasilitherium* (Cynodontia, Probainognathia) from the Late Triassic of southern Brazil. *Revista Brasileira de Paleontologia*, **8**, 25–46.

Bonaparte, J. F. & **Sues, H.-D.** 2006. A new species of *Clevosaurus* (Lepidosauria: Rhynchocephalia) from the upper Triassic of Rio Grande do Sul, Brazil. *Palaeontology*, **49**, 917–923. doi:10.1111/j.1475-49832006.00568.x

Bonaparte, J. F., **Schultz, C. L.**, **Martinelli, A. G.** & **Brea, G.** 2007. A new specimen of *Guaibasaurus candelariensis* (basal Saurischia) from the Late Triassic Caturrita Formation of southern Brazil. *Historical Biology*, **19**, 73–82. doi:10.1080/08912960600866862

Bonaparte, J. F., **Schultz, C. L.**, **Soares, M. B.** & **Martinelli, A. G.** 2010. La fauna local de Faxinal do Soturno, Triásico Tardío de Rio Grande do Sul. *Revista Brasileira de Paleontologia*, **13**, 233–246. doi:10.4072/rbp.2010.3.07

Bonaparte, J. F., **Soares, M. B.** & **Martinelli, A. G.** 2012. Discoveries in the Late Triassic of Brazil improve knowledge on the origin of mammals. *Historia Natural, Tercera Serie*, **2**, 5–30. doi:10.4072/rbp.2010.3.07

Bremer, K. 1994. Branch support and tree stability. *Cladistics*, **10**, 295–304. doi:10.1111/j.1096-0031.1994.tb00179.x

Chambi-Trowell, S. A. V., **Whiteside, D. I.** & **Benton, M. J.** 2019. Diversity in rhynchocephalian *Clevosaurus* skulls based on CT reconstruction of two Late Triassic species from Great Britain. *Acta Palaeontologica Polonica*, **64**, 41–64. doi:10.4202/app.00569.2018

Chambi-Trowell, S. A. V., **Whiteside, D. I.**, **Benton, M. J.** & **Rayfield, E. J.** 2020. Biomechanical properties of the jaws of two species of *Clevosaurus* and a reanalysis of rhynchocephalian dentary morphospace. *Palaeontology*, **63**, 919–939. doi:10.1111/pala.12493

Cisneros, J. C., & **Schultz, C. L.** 2003. *Soturnia caliodon* n. g. n. sp., a procolophonid reptile from the Upper Triassic of Southern Brazil. *Neues Jahrbuch Geologie und Paläontologie*, **227**, 365–380.

Cope, E. D. 1869. Synopsis of the extinct Batrachia, Reptilia and Aves of North America. *Transactions of the American Philosophical Society, New Series*, **14**, 1–252.

de Queiroz, K. & **J. A. Gauthier.** 2020. Lepidosauria. Pp. 1079–1085 in K. de Queiroz, P. D. Cantino & J. A. Gauthier (eds) *Phylonyms: a companion to the PhyloCode*. CRC Press, Boca Raton.

Dupret, V. 2004. The pleurosaurs: anatomy and phylogeny. *Revue de Paléobiologie*, **9**, 61–80.

Evans, S. E. 1980. The skull of a new eosuchian reptile from the Lower Jurassic of South Wales. *Zoological Journal of the Linnean Society*, **70**, 203–264.

Evans, S. E. 1981. The postcranial skeleton of the Lower Jurassic eosuchian *Gephyrosaurus bridensis*. *Zoological Journal of the Linnean Society*, **73**, 81–116.

Evans, S. E. 2008. The skull of lizards and tuatara. Pp. 1–344 in C. Gans, A. S. Gaunt & K. Adler (eds) *Biology of the Reptilia, Volume 20. Morphology H: The skull of Lepidosauria*. Society for the Study of Amphibians and Reptiles, Ithaca, New York.

Evans, S. E., **Prasad, G. V. R.** & **Manhas, B. K.** 2001. Rhynchocephalians (Diapsida: Lepidosauria) from the Jurassic Kota Formation of India. *Zoological Journal of the Linnean Society*, **133**, 309–334.

Evans, S. E. & **Borsuk-Bialynicka, M.** 2009. A small lepidosauromorph reptile from the Early Triassic of Poland. *Palaeontologia Polonica*, **65**, 179–202.

Fraser, N. C. 1982. A new rhynchocephalian from the British Upper Trias. *Palaeontology*, **25**, 709–725.

Fraser, N. C. 1988. The osteology and relationships of *Clevosaurus* (Reptilia: Sphenodontida). *Philosophical Transactions of the Royal Society B*, **321**, 125–178.

Fraser, N. C. & **Shelton, C. G.** 1988. Studies of tooth implantation in fossil tetrapods using high-resolution X-radiography. *Geological Magazine*, **125**, 117–122.

Fraser, N. C. & **Benton, M. J.** 1989. The Triassic reptiles *Brachyrhinodon* and *Polysphenodon* and the relationships of the sphenodontids. *Zoological Journal of the Linnean Society*, **96**, 413–445.

Gauthier, J. A., **Estes, R.** & **de Queiroz, K.** 1988. A phylogenetic analysis of Lepidosauromorpha. Pp. 15–98 in R. Estes & G. Pregill (eds) *Phylogenetic relationships of the lizard families*. Stanford University Press, Stanford.

Gauthier, J. A. & **de Queiroz, K.** 2020. Pan-Squamata J. A. Gauthier and K. de Queiroz, new clade name. Pp. 1087–1092 in K. de Queiroz, P. D. Cantino & J. A. Gauthier (eds) *Phylonyms: a companion to the PhyloCode*. CRC Press, Boca Raton.

Goloboff, P. A. & **Catalano, S. A.** 2016. TNT version 1.5, including a full implementation of phylogenetic morphometrics. *Cladistics*, **32**, 221–238. doi:10.1111/cla.12160

Günther, A. 1864. *The reptiles of British India*. Taylor & Francis, London, xxvii + 452 pp.

Günther, A. 1867. Contribution to the anatomy of *Hatteria* (*Rhynchocephalus*, Owen). *Philosophical Transactions of the Royal Society of London*, **157**, 595–629.

Haeckel, E. 1866. *Generelle Morphologie der Organ-ismen. Band 2: Allgemeine Entwicklungsge-schichte der Organismen*. George Reimer, Berlin, 210 pp.

Hay, J., **Sarre, S. D.**, **Lambert, D. M.**, **Allendorf, F. W.** & **Daugherty, C. H.** 2010. Genetic diversity and taxonomy: a reassessment of species designation in Tuatara (*Sphenodon*: Reptilia). *Conservation Genetics*, **11**(3), 1063–1081.

Herrera-Flores, J. A., **Stubbs, T. L.**, **Elsler, A.** & **Benton, M. J.** 2018. Taxonomic reassessment of *Clevosaurus latidens* Fraser, 1993 (Lepidosauria, Rhynchocephalia) and rhynchocephalian phylogeny based on parsimony and Bayesian inference. *Journal of Palaeontology*, **92**, 734–742. doi:10.1017/jpa.2017.136

Horn, B. L. D., **Melo, T.**, **Schultz, C. L.**, **Philipp, R. P.**, **Kloss, H. P.** & **Goldberg, K.** 2014. A new third-order sequence stratigraphic framework applied to the Triassic of the Parana Basin, Rio Grande do Sul, Brazil, based on structural, stratigraphic and paleontological data. *Journal of South American Earth Sciences*, **55**, 123–132. doi:10.1016/j.jsames.2014.07.007

Hsiou, A. S., **de França, M. A. G.** & **Ferigolo, J.** 2015. New data on the *Clevosaurus* (Sphenodontia: Clevosauridae) from the Upper Triassic of Southern Brazil. *PLoS ONE*, **10**(9), e0137523. doi:10.1371/journal.pone.0137523

Hsiou, A. S., **Nydam, R.**, **Simões, T.**, **Pretto, F.**, **Onary, S.**, **Martinelli, A. G.**, **Liparini, A.**, **Romo de Vivar Martínez, P.**, **Soares, M. B.**, **Schultz, C. L.** & **Caldwell, M.** 2019. A new clevosaurid from the Triassic (Carnian) of Brazil and the rise of sphenodontians in Gondwana. *Scientific Reports*, **9**, 11821. doi:10.1038/s41598-019-48297-9

Huelsenbeck, J. P. & **Ronquist, F.** 2001. MRBAYES: bayesian inference of phylogenetic trees. *Bioinformatics*, **17**, 754–755. doi:10.1093/bioinformatics/17.8.754

Jones, M. E. H. 2006. The Early Jurassic clevosaurs from China (Diapsida: Lepidosauria). *New Mexico Museum Natural History Science Bulletin*, **37**, 548–562.

Jones, M. E. H. & **Lappin, A. K.** 2009. Bite-force performance of the last rhynchocephalian (Lepidosauria: *Sphenodon*). *Journal of the Royal Society of New Zealand*, **39**, 71–83.

Keeble, E., **Whiteside, D. I.** & **Benton, M. J.** 2018. The terrestrial fauna of the Late Triassic Pant-y-ffynnon Quarry fissures, South Wales, UK and a new species of *Clevosaurus* (Lepidosauria: Rhynchocephalia). *Proceedings of the Geologists' Association*, **129**, 99–119.

Klein, C. G., **Whiteside, D. I.**, **de Lucas, V. S.**, **Viegas, P. A.** & **Benton, M. J.** 2015. A distinctive Late Triassic microvertebrate fissure fauna and a new species of

Clevosaurus (Lepidosauria: Rhynchocephalia) from Woodleaze Quarry, Gloucestershire, UK. *Proceedings of the Geologists' Association*, **126**, 402–416.

Langer, M. C., **Ramezani, J.** & **Da-Rosa, Á. A. S.** 2018. U-Pb age constraints on dinosaur rise from south Brazil. *Gondwana Research*, **18**, 133–140. doi:10.1016/j.gr.2018.01.005

Linnaeus, C. 1758. Description of Lacerta agilis and Lacerta algira (= Psammodromus algirus). *In Systema naturae pr regna tria naturae, secundum classes, ordines, genera, species, cum characteribus, differentiis, synonymis, locis. Tomus I. Editio decima, reformata. Laurentii Salvii, Holmiae*, pp. 203.

Lydekker, R. 1880. *Catalogue of the fossil Reptilia and Amphibia in the British Museum of Natural History. Part 1.* Order of the Trustees, London.

Maisano, J. 2001. *Sphenodon punctatus*, digital morphology. Updated at: http://digimorph.org/specimens/Sphenodon_punctatus/adult/, accessed 22 April 2018.

Martinelli, A. G., **Bonaparte, J. F.**, **Schultz, C. L.** & **Rubert, R.** 2005. A new tritheledontid (Therapsida, Eucynodontia) from the Late Triassic of Rio Grande do Sul (Brazil) and its phylogenetic relationships among carnivorous non-mammalian eucynodonts. *Ameghiniana*, **42**, 191–208.

Martinelli, A. G., **Eltink, E.**, **Da-Rosa, Á. A. S.** & **Langer, M. C.** 2017. A new cynodont from the Santa Maria Formation, south Brazil, improves Late Triassic probainognathian diversity. *Papers in Palaeontology*, **3**, 401–423. doi:10.1002/spp2.1081

Martinelli, A. G., **Escobar, J. A.**, **Francischini, H.**, **Kerber, L.**, **Müller, R. T.**, **Rubert, R.**, **Schultz, C. L.** & **Da-Rosa, Á. A. S.** 2020. New record of a stahleckeriid dicynodont (Therapsida, Dicynodontia) from the Late Triassic of southern Brazil and biostratigraphic remarks on the *Riograndia* Assemblage Zone. *Historical Biology*. doi:10.1080/08912963.2020.1850715

Martínez, R. N., **Apaldetti, C.**, **Alcober, O. A.**, **Correa, G. A.** & **Abelín, D.** 2013. Vertebrate succession in the Ischigualasto Formation. *Memoir of the Vertebrate Paleontology*, **12**, 10–30. doi:10.1080/02724634.2013.818546

Nopcsa, F. 1923. Die Familien der Reptilen. In W. Soergel (ed.) *Fortschritte der Geologie und Palaeontologie. Volume 2.* Borntraeger, Berlin, 210 pp.

Nopcsa, F. 1928. Palaeontological notes on reptiles. *Geologica Hungarica, Series Palaeontologia*, **1**(1), 1–84.

O'Brien, A., **Whiteside, D. I.** & **Marshall, J. E. A.** 2018. Anatomical study of two previously undescribed specimens of *Clevosaurus hudsoni* (Lepidosauria: Rhynchocephalia) from Cromhall Quarry, UK, aided by computed tomography, yields additional information on the skeleton and hitherto undescribed bones. *Zoological Journal of the Linnean Society*, **183**, 163–195. doi:10.1093/zoolinnean/zlx087

Oliveira, T. V., **Martinelli, A. G.** & **Soares, M. B.** 2011. New material of *Irajatherium hernandezi* Martinelli, Bonaparte, Schultz & Rubert 2005 (Eucynodontia, Tritheledontidae) from the Upper Triassic (Caturrita Formation, Paraná Basin) of Brazil. *Paläontologische Zeitschrift*, **85**, 67–82.

O'Reilly, J. E. & **Donoghue, P. C. J.** 2018. The efficacy of consensus tree methods for summarizing phylogenetic relationships from a posterior sample of trees estimated from morphological data. *Systematic Biology*, **67**, 354–362.

Philippi, R. A. & **Landeck, L.** 1861. Neue Wirbelthiere von Chile. *Archiv für Naturgeschichte*, **27**, 289–301.

Rasmussen, T. E., & **Callison, G.** 1981. A new herbivorous sphenodontid (Rhynchocephalia: Reptilia) from the Jurassic of Colorado. *Journal of Paleontology*, **55**, 1109–1116.

Rauhut, O. W. M., **Heyng, A. M.**, **López-Arbarello, A.** & **Hecker, A.** 2012. A new rhynchocephalian from the Late Jurassic of Germany with a dentition that is unique amongst tetrapods. *PLoS ONE*, **7**(10), e46839. doi:10.1371/journal.pone.oo46839

Robinson, P. L. 1962. Gliding lizards from the Upper Keuper of Great Britain. *Proceedings of the Geological Society of London*, **1601**, 137–146.

Romo de Vivar Martínez, P. R. & **Soares, M. B.** 2015. Dentary morphological variation in *Clevosaurus brasiliensis* (Rhynchocephalia, Clevosauridae) from the Upper Triassic of Rio Grande do Sul, Brazil. *PLoS ONE*, **10**(3), e0119307. doi:10.1371/journal.pone.0119307

Romo-de-Vivar-Martínez, P. R., **Martinelli, A. G.**, **Paes Neto, V. D.**, **Scartezini, C. A.**, **Lacerda, M. B.**, **Rodrigues, C. N.**, & **Soares, M. B.** 2019. New rhynchocephalian specimen in the Late Triassic of southern Brazil and comments on the palatine bone of Brazilian rhynchocephalians. *Historical Biology*, **33**(2), 209–217. doi:10.1080/08912963.2019.1602616

Romo de Vivar, P. R., **Martinelli, A. G.**, **Hsiou, A. S.** & **Soares, M. B.** 2020a. A new rhynchocephalian from the Late Triassic of Southern Brazil enhances eusphenodontian diversity. *Journal of Systematic Palaeontology*, **18**, 1103–1126. doi:10.1080/14772019.2020.1732488

Romo de Vivar, P. R., **Martinelli, A. G.**, **Fonseca, P. H. M.** & **Soares, M. B.** 2020b. To be or not to be: the hidden side of *Cargninia enigmatica* and other puzzling remains of Lepidosauromorpha from the Upper Triassic of Brazil. *Journal of Vertebrate Paleontology*, **40**, e1828438. doi:10.1080/02724634.2020.1828438

Romo-de-Vivar-Martínez, P. R., **Martinelli, A. G.**, **Paez Neto, V. D.**, **Scartezini, C.**, **Lacerda, M. B.**, **Rodrigues, C.** & **Soares, M. B.** 2021. New rhynchocephalian specimen in the Late Triassic of southern Brazil and comments on the palatine bone of Brazilian rhynchocephalians. *Historical Biology*, **33**, 209–217.

Ronquist, F., **Teslenko, M.**, **Mark, P.**, **Ayres, D.**, **Darling, A.**, **Hohna, S.**, **Larget, B.**, **Lui, L.**, **Suchard, M.** & **Huelsenbeck, J.** 2012. MrBayes 3.2: efficient Bayesian phylogenetic inference and model choice across a large model space. *Systematic Biology*, **61**, 539–542. doi:10.1093/sysbio/sys029

Säilä, L. K. 2005. A new species of the sphenodontians reptiles *Clevosaurus* from the Lower Jurassic of South Wales. *Palaeontology*, **48**, 817–831. doi:10.1111/j.1475-4983.2005.00486.x

Schultz, C. L., **Martinelli, A. G.**, **Soares, M. B.**, **Pinheiro, F.**, **Kerber, L.**, **Horn, B.**, **Pretto, F.**, **Müller, R.** & **Melo, T.** 2020. Triassic faunal successions of the Paraná Basin, southern Brazil. *Journal of South American Earth Sciences*, **104**, 102846. doi:10.1016/j.jsames.2020.102846

Simões, T. R., **Caldwell, M. W.** & **Pierce, S. E.** 2020. Sphenodontian phylogeny and the impact of model choice in Bayesian morphological clock estimates of divergence

times and evolutionary rates. *BMC Biology*, **18**, 191. 10. 1186/s12915-020-00901-5.

Soares, M. B., Schultz, C. L. & **Horn, B. L. D.** 2011. New information on *Riograndia guaibensis* Bonaparte, Ferigolo & Ribeiro, 2001 (Eucynodontia, Tritheledontidae) from the Late Triassic of southern Brazil: anatomical and biostratigraphic implications. *Anais da Academia Brasileira de Cíencias*, **83**, 329–354. doi:10.1590/S0001-37652011000100021

Soares, M. B., **Vecchia, D.**, **Schultz. C. F.**, & **Alexander, K.** 2013. On the supposed pterosaurian nature of *Faxinalipterus minima* Bonaparte *et al.* (2010) from the Upper Triassic of Rio Grande do Sul, Brazil. Pp. 95–97 in J. Sayão Manso, F. Costa Rodrigues, R. A. M. Bantim, & A. W. A. Kellner (eds) *International Symposium on Pterosaurs, Rio Ptero 2013, Short Communications*. Universidade Federal Do Rio De Janeiro, Rio De Janeiro.

Sues, H.-D., **Shubin, N. H.** & **Olsen, P. E.** 1994. A new sphenodontian (Lepidosauria: Rhynchocephalia) from the McCoy Brook Formation (Lower Jurassic) of Nova Scotia, Canada. *Journal of Vertebrate Paleontology*, **14**, 327–340.

Swinton, W. E. 1939. A new Triassic rhynchocephalian from Gloucestershire. *Annals and Magazine of Natural History: Zoology, Botany, and Geology*, **4**, 591–594.

Swofford, D. L. 2002. *PAUP*. Phylogenetic analysis using parsimony (*and other methods), v. 4*. Sunderland: Sinauer Associates.

Whiteside, D. I. 1986. The head skeleton of the Rhaetian sphenodontid *Diphydontosaurus avonis* gen. et sp. nov. and the modernizing of a living fossil. *Philosophical Transactions of the Royal Society of London Series B*, **312**, 379–430.

Williston, S. 1925. *The osteology of the reptiles*. Harvard University Press, Cambridge (USA, 281 pp.

Wu, X. -C. 1994, Late Triassic–Early Jurassic sphenodontians from China and the phylogeny of the Sphenodontia. Pp. 38–69 in N. C. Fraser & H.-D. Sues (eds) *In the shadow of the dinosaurs*. Cambridge University Press, Cambridge.

Zerfass, H., **Lavina, E. L.**, **Schultz, C. L.**, **Garcia, A. J. V.**, **Faccini, U. F.** & **Chemale, F. Jr.** 2003. Sequence stratigraphy of continental Triassic strata of southern-most Brazil: a contribution to southwestern Gondwana palaeogeography and palaeoclimate. *Sedimentary Geology*, **161**, 85–105. doi:10.1016/S0037-0738(02)00397-4

Associate Editor: Jennifer Olori